ИТМО

А.П. Алоджанц, А.Ю. Баженов, М.М. Никитина, С.В. Осипов, Д.В. Царёв

INTERACTION OF RADIATION WITH MATTER: GUIDELINES FOR PRACTICAL WORK

Санкт-Петербург
2022

МИНИСТЕРСТВО НАУКИ И ВЫСШЕГО ОБРАЗОВАНИЯ
РОССИЙСКОЙ ФЕДЕРАЦИИ

УНИВЕРСИТЕТ ИТМО

Алоджанц А.П., Баженов А.Ю., Никитина М.М., Осипов С.В., Царёв Д.В.

INTERACTION OF RADIATION WITH MATTER: GUIDELINES FOR PRACTICAL WORK

РЕКОМЕНДОВАНО К ИСПОЛЬЗОВАНИЮ В УНИВЕРСИТЕТЕ ИТМО
по направлению подготовки 16.04.01 Техническая физика
Образовательной программы магистратуры Лазерные и синхротронные технологии мегасайенс / Megascience laser and synchrotron technologies в качестве учебного пособия для реализации основных профессиональных образовательных программ высшего образования магистратуры

ИТМО

Санкт-Петербург

2022

Алоджанц А.П., Баженов А.Ю., Никитина М.М., Осипов С.В, Царёв Д.В., INTERACTION OF RADIATION WITH MATTER: GUIDELINES FOR PRACTICAL WORK – СПб: Университет ИТМО, 2022. – 52 с.

Рецензент:

Рождественский Юрий Владимирович, доктор физико-математических наук, профессор (квалификационная категория "ординарный профессор") факультета фотоники Университета ИТМО.

Учебное пособие разработано при поддержке Министерства науки и высшего образования Российской Федерации (соглашение № 075-15-2021-1349) в соответствии с программой дисциплины "Взаимодействие излучения с веществом / Interaction of Radiation with Matter предназначенной для студентов, обучающихся но направлению 16.04.01 "Техническая физика" Образовательной программы магистратуры "Лазерные и синхротронные технологии мегасайенс / Megascience laser and synchrotron technologies". Пособие содержит краткий (вводный) теоретический материал, который посвящен квантованию электромагнитного излучения и его свойствам, основным квантовым моделям взаимодействия излучения с веществом, таким как: квазиклассическая модель Раби-осцилляций, модель Джейнса-Каммингса, модель одетых состояний и поляритонная модель. В пособии собран большой набор вопросов и задач для практических занятий, представлены рекомендации по их решению и оформлению.

ИТМО

Университет ИТМО – ведущий вуз России в области информационных и фотонных технологий, один из немногих российских вузов, получивших в 2009 году статус национального исследовательского университета. С 2013 года Университет ИТМО – участник программы повышения конкурентоспособности российских университетов среди ведущих мировых научно-образовательных центров, известной как проект «5 в 100». Цель Университета ИТМО – становление исследовательского университета мирового уровня, предпринимательского по типу, ориентированного на интернационализацию всех направлений деятельности.

Content

1 Introduction

Interaction of radiation with matter represents an extensive direction in current scientific research, engineering, and industry. It lies at the interfaces of laser and quantum physics, condensed matter and information science, chemistry, biophotonics and medicine. Monochromatic directed laser radiation represents an indispensable tool for studying crucial physical and chemical properties of matter. Recently, novel promising sources of X-ray laser radiation have been created in the framework of X-Ray Free-Electron Laser (XFEL) megascience lab. At the same time, interaction of radiation with matter represents a keystone prerequisite for progress in quantum technologies.

The course "Interaction of radiation with matter" at ITMO aims to introduce master students to the main current methods and approaches of research and engineering in this area. The course bridges the gap between standard quantum mechanics and such engineering courses as nonlinear and quantum optics taught at undergraduate level.

The purpose of this guideline is to provide students with theoretical knowledge and practical skills in learning and understanding the course. Although the topic of interaction of light with matter is quite extensive, there are only a few models that can be accurately solved. Here, we examine such models in detail.

The guideline topics encompass the interaction of a quantum two-level system with a classical laser field, features of a quantized electromagnetic field, the dressed states model of atom-light interaction, the Jaynes–Cummings model as a seminal quantum model of the interaction of radiation with matter and simple quantum models of bosonic quasiparticles, such as microcavity exciton-polaritons.

Completed courses in quantum mechanics and optics are prerequisites to master this course. In particular, master students are required to be familiar with the Dirac formulation of quantum theory in Hilbert space that is used in the guideline without specification. Special attention is paid to the problems aimed at understanding and synthesising the material.

We are grateful to our colleagues at ITMO for useful comments and suggestions.

2 Quantum States of Electromagnetic Field

In this Section we briefly consider the quantization of electromagnetic (e.m.) field and its basic quantum properties.

2.1 Quantization of free electromagnetic field

2.1.1 Preliminary remarks

Quantization of free electromagnetic field represents one of keystone problems in quantum theory. The rigorous quantization procedure is cumbersome and requires a Lorentz-invariant form based on a vector-potential approach. The reader can find it in [1]. However, for practical purposes establishing key results of such a quantization is enough. Here, we propose a schematic physical picture of the e.m. field quantization.

The aim of practically significant procedure of e.m. field quantization is to find variables, which could describe its quantum properties. It is important to consider that momentum $p \equiv p_x$ and relevant position x (here we discuss the 1D case for simplicity) are not directly appropriate for the field quantization procedure, although they are the basis of quantization in quantum mechanics. A photon freely propagating in vacuum with speed c, as a quantum particle of radiation, has a certain momentum (wave vector $\mathbf{k}$) but does not have a precisely defined position. Thus, we need to find field variables, measurable experimentally, which would be some analogs for the momentum and position in quantum mechanics. In this regard, the classical harmonic oscillator represents a suitable model (thereafter we examine 1D harmonic oscillator features), see Fig. 1.

We consider a linearly polarized along X-axis e.m. field confined within an empty cubic cavity of volume $V = L^3$, as shown in Fig. 1. In fact, we deal with the standing wave possessing nodes at $Z = 0$ and $Z = L$. Note, in the original procedure of field quantization we assume that L is large enough.

The determining of e.m. field in the cavity allows to compare its mode properties with classical harmonic oscillator features. In this case, we assume that energy of harmonic oscillator E_{cl} is equivalent to energy of the field E_F in the cavity. As a result, it is possible to obtain an important relation between oscillator momentum p, position x and amplitude $\mathcal{E}$ of the classical e.m. field, as shown in Fig. 1.

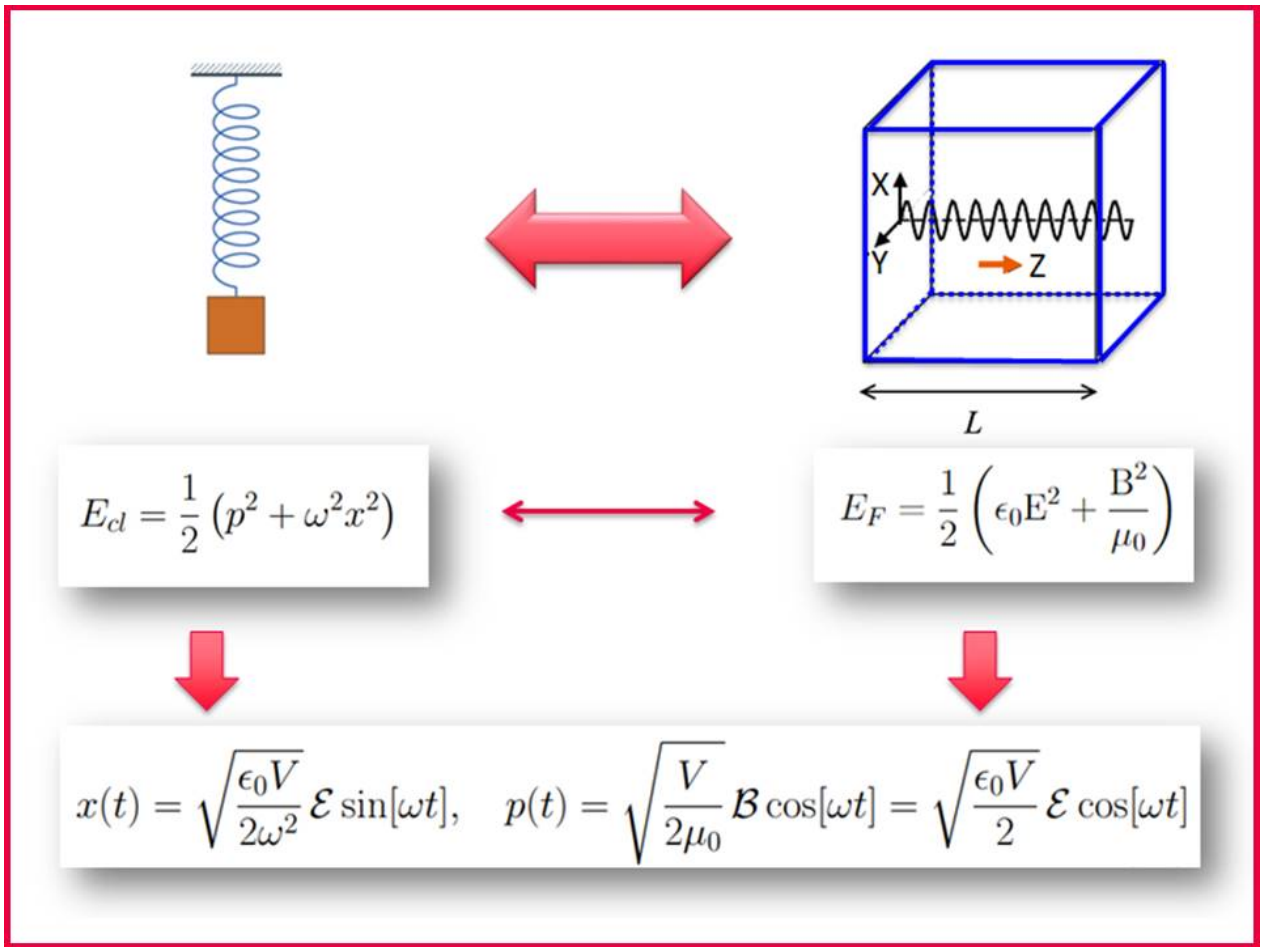

Fig. 1: Scheme of relation for physical characteristics of harmonic oscillator with mass $m = 1$ and e.m. field mode in the cavity of volume $V = L^3$ underlying the core of quantization procedure. The e.m. field represents a standing wave oscillating with angular frequency ω inherent to some harmonic oscillator frequency. The second row demonstrates the required mathematical equivalence between energy of the classical harmonic oscillator E_{cl} and energy E_F of e.m. field in the cavity. $\mathrm{E} = \mathcal{E}\sin[kz]\sin[\omega t]$ and $\mathrm{B} = \mathcal{B}\cos[kz]\cos[\omega t]$ are time-dependent electric and magnetic fields, which are solutions of relevant Maxwell equations; ϵ_0 is the electric permittivity and μ_0 is the magnetic permeability of the vacuum. The third row establishes a formal connection between oscillator momentum p and position x with relevant e.m. field variables, which are electric ($\mathcal{E}$) and magnetic ($\mathcal{B} = \mathcal{E}/c$) field amplitudes

2.1.2 Second quantization procedure

The quantization of e.m. field is based on the idea of correspondence between basic features of a quantized field mode in the cavity and quantum harmonic

oscillator having angular frequency ω and definite energy E, as it takes place in the classical approach, cf. Fig. 1.

We start with the *second quantization procedure* performed with quantum harmonic oscillator variables. In quantum mechanics its momentum $\hat{p}$ and position $\hat{x}$ are Hermitian operators, which satisfy canonical commutation relation

$$[\hat{x}, \hat{p}] = \hat{x}\hat{p} - \hat{p}\hat{x} = i\hbar. \tag{1}$$

As a result, the oscillator momentum and position obey Heisenberg uncertainty relation

$$\sigma_x \sigma_p \geq \frac{\hbar}{2}, \tag{2}$$

where $\sigma_x^2 \equiv \left\langle \hat{x}^2 \right\rangle - \left\langle \hat{x} \right\rangle^2$ and $\sigma_p^2 \equiv \left\langle \hat{p}^2 \right\rangle - \left\langle \hat{p} \right\rangle^2$ are variances of position and momentum observables, respectively.

The energy of quantum harmonic oscillator may be obtained from the eigenstates and eigenvalues equation established for quantum Hamiltonian of harmonic oscillator

$$\hat{H} = \frac{\hat{p}^2}{2m} + \frac{m\omega^2 \hat{x}^2}{2}. \tag{3}$$

For simplicity, further we assume that the mass of oscillator is $m = 1$.

In quantum theory it is known that (3) possesses discrete energy spectrum E_n that looks like (cf. [2])

$$E_n = \left(n + \frac{1}{2} \right) \hbar\omega, \tag{4}$$

where $n = 0,1,2,...,\infty$ is a quantum number. The eigenstates of Hamiltonian (3) are relevant to the Hermite polynomials.

The energy levels (the right column) and corresponding set of quantum states (the left column) are shown in Fig. 2. Notably, the ground state of quantum oscillator with $n = 0$ possesses a finite (non-zero) energy and is characterized by the Gaussian wave function.

In the second quantization formalism we can introduce new variables $\hat{a}$, $\hat{a}^\dagger$, which are relevant to the x and p variables, see e.g. [3],

$$\hat{a} = \frac{1}{\sqrt{2\hbar\omega}} \left(\omega\hat{x} + i\hat{p} \right), \tag{5a}$$

$$\hat{a}^\dagger = \frac{1}{\sqrt{2\hbar\omega}} \left(\omega\hat{x} - i\hat{p} \right). \tag{5b}$$

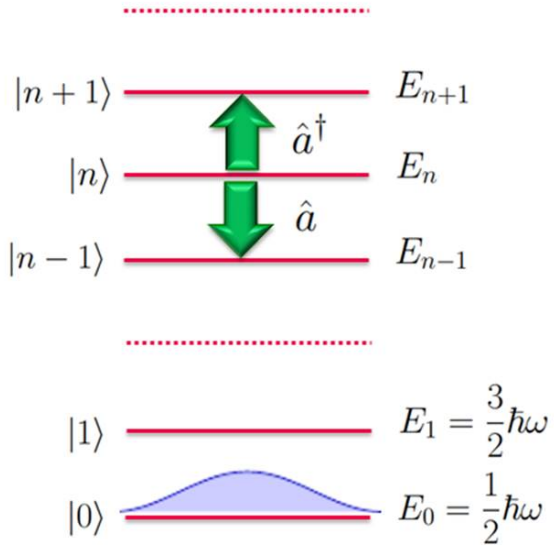

Fig. 2: Energy levels for quantum harmonic oscillator with angular frequency ω. Annihilation, $\hat{a}$, and creation, $\hat{a}^\dagger$, operators subtract from and add to any given state $|n\rangle$ one quanta energy $\hbar\omega$. The shaded region illustrates the Gaussian wave function that corresponds to the oscillator ground (vacuum) state

In quantum theory operators defined in (5) are called ***annihilation***, $\hat{a}$, and ***creation***, $\hat{a}^\dagger$, ***operators***, respectively. They are ***non-Hermitian*** and obey commutation relation

$$\left[\hat{a}, \hat{a}^\dagger\right] \equiv \hat{a}\hat{a}^\dagger - \hat{a}^\dagger\hat{a} = 1. \tag{6}$$

From (5) we can obtain inverse transformations

$$\hat{x} = \sqrt{\frac{\hbar}{2\omega}}\left(\hat{a} + \hat{a}^\dagger\right), \tag{7a}$$

$$\hat{p} = i\sqrt{\frac{\hbar\omega}{2}}\left(\hat{a}^\dagger - \hat{a}\right). \tag{7b}$$

Substituting (7a), (7b) into (3) we obtain quantum harmonic oscillator Hamiltonian $\hat{H}$ in its second quantization form,

$$\hat{H} = \hbar\omega\left(\hat{a}^\dagger\hat{a} + \frac{1}{2}\right). \tag{8}$$

Operator

$$\hat{n} \equiv \hat{a}^\dagger \hat{a} \tag{9}$$

is called a particle number operator.

Energy spectrum E_n (see (4)) represents the eigenenergy of Hamiltonian $\hat{H}$ specified in (8), if we consider ***Fock states*** $|n\rangle$, which are defined by the following rules:

$$\hat{a}\,|n\rangle = \sqrt{n}\;|n-1\rangle\,; \tag{10a}$$

$$\hat{a}^\dagger\,|n\rangle = \sqrt{n+1}\;|n+1\rangle\,. \tag{10b}$$

Throughout this work we use the Dirac notation for quantum state representation, see e.g. [4] for details.

Fock states represent an orthonormal basis in the Hilbert space; condition is satisfied:

$$\langle m|n\rangle = \delta_{mn} \equiv \begin{cases} 1, & \text{if } m = n; \\ 0, & \text{if } m \neq n. \end{cases} \tag{11}$$

Thus, from (10) it follows that the annihilation operator, $\hat{a}$, subtracts one quanta energy, whereas the creation operator, $\hat{a}^\dagger$, adds one quanta, see Fig. 2.

Fock states, which obey (11), may be established as column vectors in the form:

$$|0\rangle = \begin{pmatrix} 1 \\ 0 \\ 0 \\ \vdots \end{pmatrix}, \quad |1\rangle = \begin{pmatrix} 0 \\ 1 \\ 0 \\ \vdots \end{pmatrix}, \quad |2\rangle = \begin{pmatrix} 0 \\ 0 \\ 1 \\ \vdots \end{pmatrix}, \quad ... \tag{12}$$

We can also represent the annihilation ($\hat{a}$) and creation ($\hat{a}^\dagger$) operators specified in (10) in the matrix form as

$$\hat{a} = \begin{pmatrix} 0 & \sqrt{1} & 0 & 0 & . \\ 0 & 0 & \sqrt{2} & 0 & . \\ 0 & 0 & 0 & \sqrt{3} & . \\ . & . & . & 0 & . \end{pmatrix}; \tag{13a}$$

$$\hat{a}^\dagger = \begin{pmatrix} 0 & 0 & 0 & 0 & . \\ \sqrt{1} & 0 & 0 & 0 & . \\ 0 & \sqrt{2} & 0 & 0 & . \\ . & . & . & 0 & . \end{pmatrix}. \tag{13b}$$

Apparently, Eqs. (13) demonstrate the non-diagonal form for the annihilation and creation operators in the Fock basis.

The important limiting case of (10), which requires additional definition, is vacuum state $|0\rangle$ that corresponds to the ground state of harmonic oscillator with $n = 0$. It may be described as

$$\hat{a}\,|0\rangle = 0. \tag{14}$$

From (10) it immediately follows that $|n\rangle$ is the eigenstate of particle number operator $\hat{n}$, i.e.

$$\hat{a}^\dagger \hat{a}\,|n\rangle = \hat{a}^\dagger \sqrt{n}\,|n-1\rangle = \sqrt{n}\;\hat{a}^\dagger\,|n-1\rangle = n\,|n\rangle\,. \tag{15}$$

Thus, we can conclude that mean value

$$n = \left\langle n \left| \hat{a}^\dagger \hat{a} \right| n \right\rangle \tag{16}$$

represents the average number of particles. In this case, from (8) we obtain

$$\left\langle n \left| \hat{H} \right| n \right\rangle = \left(n + \frac{1}{2} \right) \hbar\omega, \tag{17}$$

which immediately reproduces seminal result (4) obtained for the energy of quantum harmonic oscillator.

Thus, now we can use operators defined in (5) and states from (10) and (14) to determine quantum harmonic oscillator properties instead of its momentum and position.

2.2 Quantized electromagnetic field properties

2.2.1 Field operators

Let us consider the quantization of e.m. field in the cavity with volume V. The quantization procedure presumes introduction of photon annihilation $\hat{a}$ and creation $\hat{a}^\dagger$ operators instead of classical (complex) field amplitudes $\mathcal{E}$ and $\mathcal{E}^*$, respectively, see e.g. [3]. In this case, quantum theory proposes a plane-wave single-mode field operator that may be represented as (cf. [5])

$$\hat{\mathbf{E}}\,(\mathbf{r},t) = i \left(\frac{\hbar\omega}{2\varepsilon_0 V} \right)^{\frac{1}{2}} \mathbf{e}_x \left[\hat{a}\, e^{i\mathbf{kr} - i\omega t} - \hat{a}^\dagger\, e^{-i\mathbf{kr} + i\omega t} \right], \tag{18}$$

where V is a quantization volume, $\mathbf{e}_x$ is a unit vector of polarization. In (18) $\sqrt{\frac{\hbar\omega}{2\varepsilon_0 V}}$ is a constant that may be obtained if we account field Hamiltonian and relevant photon energy in the forms of (8) and (4), respectively.

The quantum theory (see e.g. [3]) also shows that electric field operator $\hat{\mathbf{E}}$ in a more general (multimode) case is given as

$$\hat{\mathbf{E}}\left(\mathbf{r},t\right) = i\sum_{\mathbf{k}s}\left(\frac{\hbar\omega_k}{2\varepsilon_0 V}\right)^{\frac{1}{2}}\mathbf{e}_{\mathbf{k}s}\left[\hat{a}_{\mathbf{k}s}\,e^{i(\mathbf{kr}-\omega_k t)} - \hat{a}^{\dagger}_{\mathbf{k}s}\,e^{-i(\mathbf{kr}-\omega_k t)}\right], \tag{19}$$

where $\mathbf{e}_{\mathbf{k}s}$ is a polarization vector. Operators $\hat{a}_{\mathbf{k}s}$, $\hat{a}^{\dagger}_{\mathbf{k}s}$ in (19) are relevant to the annihilation and creation of a photon with wave vector $\mathbf{k}$ and polarization $\mathbf{e}_{\mathbf{k}s}$. At the same time, magnetic field operator $\hat{\mathbf{B}}$ reads as

$$\hat{\mathbf{B}}\left(\mathbf{r},t\right) = \frac{i}{c}\sum_{\mathbf{k}s}\left(\mathbf{K}\times\mathbf{e}_{\mathbf{k}s}\right)\left(\frac{\hbar\omega_k}{2\varepsilon_0 V}\right)^{\frac{1}{2}}\mathbf{e}_{\mathbf{k}s}\left[\hat{a}_{\mathbf{k}s}\,e^{i(\mathbf{kr}-\omega_k t)} - \hat{a}^{\dagger}_{\mathbf{k}s}\,e^{-i(\mathbf{kr}-\omega_k t)}\right], \tag{20}$$

where $\mathbf{K} \equiv \mathbf{k}/\left|\mathbf{k}\right|$.

Rigorously speaking, field operators in (19), (20) may be obtained from the vector-potential solutions of Maxwell equations, see e.g. [1].

The annihilation and creation operators appearing in (19), (20) satisfy bosonic commutation relations (cf. (6))

$$[\hat{a}_{\mathbf{k}s},\,\hat{a}_{\mathbf{k}'s'}] = 0 = \left[\hat{a}^{\dagger}_{\mathbf{k}s},\,\hat{a}^{\dagger}_{\mathbf{k}'s'}\right]; \tag{21}$$

$$\left[\hat{a}_{\mathbf{k}s},\,\hat{a}^{\dagger}_{\mathbf{k}'s'}\right] = \delta_{\mathbf{k}\mathbf{k}'}\,\delta_{ss'}. \tag{22}$$

Thus, in the multimode case e.m. field may be recognized as the sum of *independent* harmonic oscillators described by a set of annihilation ($\hat{a}_{\mathbf{k}s} \equiv \hat{a}_j$) and creation ($\hat{a}^{\dagger}_{\mathbf{k}s} \equiv \hat{a}^{\dagger}_j$) operators, respectively. The total Hamiltonian of the multimode field is

$$\hat{H} = \hbar\sum_j \omega_j\left(\hat{n}_j + \frac{1}{2}\right), \tag{23}$$

where $\hat{n}_j \equiv \hat{a}^{\dagger}_j\hat{a}_j$ is a particle number operator for the j-th oscillator.

Quantum state $|\psi\rangle$ of the multimode field with some finite (or infinite) number of independent modes represents a *tensor product state* that looks like

$$|\psi\rangle \equiv |n_1\rangle\otimes|n_2\rangle\otimes\ldots|n_{j-1}\rangle\otimes|n_j\rangle\otimes|n_{j+1}\rangle\otimes\ldots\,. \tag{24}$$

Further, we omit sign $\otimes$ for brevity.

The rules of annihilation and creation operators action on the state $|\psi\rangle$ may be now defined as

$$\hat{a}_j |\psi\rangle = \sqrt{n_j}\ |n_1\rangle |n_2\rangle ... |n_{j-1}\rangle |n_j - 1\rangle |n_{j+1}\rangle ... ; \tag{25a}$$

$$\hat{a}_j^\dagger |\psi\rangle = \sqrt{n_j + 1}\ |n_1\rangle |n_2\rangle ... |n_{j-1}\rangle |n_j + 1\rangle |n_{j+1}\rangle ... . \tag{25b}$$

Thus, any j-th annihilation (or creation) operator acts only on the state relevant to the same, j-th mode of the e.m. field. Eqs. (23), (25) imply the energy of multimode e.m. field given as

$$E = \hbar \sum_j \omega_j \left(n_j + \frac{1}{2} \right). \tag{26}$$

The energy,

$$E_0 = \frac{1}{2} \sum_j \hbar\omega_j, \tag{27}$$

is called *zero-point energy* of harmonic oscillators. For infinite number of modes E_0 diverges, which represents an essential difficulty for the quantization procedure in theory [1]. We will discuss it further.

2.2.2 Dipole approximation

Spatial variation of the field over the spatial dimensions of the medium (atoms, quantum dots, etc.) may be negligible in many problems of matter – field interaction. In particular, in the *optical* domain for wavelength λ the condition is still satisfied

$$\frac{\lambda}{2\pi} = \frac{1}{|\mathbf{k}|} \gg |\mathbf{r}_{at}|, \tag{28}$$

where $|\mathbf{r}_{at}|$ is a characteristic length of atom localization. As a result, one can assume that $e^{\pm i\mathbf{kr}} \approx 1 \pm i\mathbf{kr} \simeq 1$. In this limit for the single-mode (linearly polarized in X direction) quantized field we can use

$$\hat{\mathrm{E}}(t) = i \left(\frac{\hbar\omega}{2\varepsilon_0 V} \right)^{\frac{1}{2}} \left[\hat{a} e^{-i\omega t} - \hat{a}^\dagger e^{i\omega t} \right]. \tag{29}$$

This is so-called dipole approximation, which allows to neglect spatial effects under the matter-field interaction within this guideline. In particular, for visible light wavelength λ is about μm. We can accept the estimation of $|\mathbf{r}_{at}|$ of the order of 0.053 nm that is relevant to the Bohr radius. Thus, the dipole approximation works with a margin of several orders of magnitude.

2.2.3 Quadrature operators for single-mode field

Equations (7a), (7b) established for the quantum harmonic oscillator allow to introduce dimensionless position-like ($\hat{X}_1$) and momentum-like ($\hat{X}_2$) *Hermitian quadrature operators* for the single-mode photonic field as follows

$$\hat{X}_1 = \frac{1}{2}\left(\hat{a} + \hat{a}^\dagger\right); \tag{30a}$$

$$\hat{X}_2 = \frac{1}{2i}\left(\hat{a} - \hat{a}^\dagger\right). \tag{30b}$$

In particular, electric field operator (29) can be obtained in terms of (30a), (30b) in the form

$$\hat{E}(t) \simeq \hat{X}_1 \cos\left[\omega t\right] + \hat{X}_2 \sin\left[\omega t\right]. \tag{31}$$

From (31) it is clearly seen that the $\hat{X}_1$ and $\hat{X}_2$ operators are out-of-phase with each other by $\pi/2$. They satisfy the commutation relation,

$$\left[\hat{X}_1,\ \hat{X}_2\right] = \frac{i}{2}, \tag{32}$$

which represents the direct consequence of (1). From (32) it follows that

$$\left\langle \left(\Delta\hat{X}_1\right)^2 \right\rangle \left\langle \left(\Delta\hat{X}_2\right)^2 \right\rangle \geq \frac{1}{16}, \tag{33}$$

where $\left\langle \left(\Delta\hat{X}_{1,2}\right)^2 \right\rangle$ is variance of quadrature $\hat{X}_{1,2}$.

Heisenberg uncertainty relation (33) manifests the impossibility of simultaneous and exact measurement of the $\hat{X}_{1,2}$ quadratures for the quantum e.m. field. Below we will specify (33) for some practically significant states, which represent useful tool in quantum optics.

2.3 Fock states of electromagnetic field

First, let us examine ***vacuum state***, which we have already introduced in (14). It represents a particular case of Fock state $|n\rangle$ with $n = 0$.

Arbitrary dimension Fock state $|n\rangle$ may be obtained from the vacuum by using a set of creation operators, i.e.

$$|n\rangle = \frac{\left(\hat{a}^\dagger\right)^n}{\left(n!\right)^{1/2}}\left|0\right\rangle, \quad n = 0,1,2... \,. \tag{34}$$

In quantum optics, $|0\rangle$ represents the state with zero number of photons in average. Eq. (14) means that there are no states below $|0\rangle$. From (4) we can see that the vacuum state possesses nonzero energy $E_0 = \hbar\omega/2$.

The energy of vacuum state is infinite for the multimode radiation, for which we have (c.f. (27))

$$E_0 = \int_0^{+\infty} \frac{\hbar V \omega^3}{2\pi^2 c^3} d\omega. \tag{35}$$

The transition from discrete (27) to continuous version (35) may be performed by replacing the sum over the modes by a relevant integral defined in the frequency domain if the number of modes possessing different frequencies is large enough, cf. [3].

Eq. (35) clearly demonstrates the divergence of zero-point energy. However, in real-world experiments we usually obtain energy difference, which remains finite. On the other hand, the detectors, which we use in real-world experiments, possess a finite spectral bandwidth, which helps us to examine (35) within the finite (spectral) limits.

Now we examine fluctuations of the e.m. field in the vacuum state. From definitions (30a), (30b), and (14) we have $\langle 0|\hat{X}_1|0\rangle = \langle 0|\hat{X}_2|0\rangle = 0$, but

$$\left\langle \left(\Delta \hat{X}_1\right)^2 \right\rangle_{vac} = \left\langle \left(\Delta \hat{X}_2\right)^2 \right\rangle_{vac} = \frac{1}{4}. \tag{36}$$

Thus, from (36) it follows that vacuum state $|0\rangle$ minimizes Heisenberg uncertainty relation (33).

Let us consider *Fock states* defined in (10), (17) for arbitrary (non-zero) n. The Fock states represent a complete set of basis vectors in the Hilbert space, that is

$$\sum_{n=0}^{\infty} |n\rangle \langle n| = \hat{\mathbf{1}}. \tag{37}$$

With (10) and (17) it is easy to show that

$$\left\langle n \left| \hat{X}_1 \right| n \right\rangle = \left\langle n \left| \hat{X}_2 \right| n \right\rangle = 0. \tag{38}$$

However, the second moments are non-zero and may be computed as

$$\left\langle n \left| \hat{X}_1^2 \right| n \right\rangle = \frac{1}{4} \left\langle n \left| \hat{a}^2 + \hat{a}^{\dagger 2} + \hat{a}^\dagger \hat{a} + \hat{a}\hat{a}^\dagger \right| n \right\rangle = \frac{1}{4} \left\langle n \left| \hat{a}^2 + \hat{a}^{\dagger 2} + 2\hat{a}^\dagger \hat{a} + 1 \right| n \right\rangle = \frac{1}{4} + \frac{1}{4} \left(\langle n \left| \hat{a}^2 | n \right\rangle + \langle n \left| \hat{a}^{\dagger 2} | n \right\rangle + 2 \left\langle n \left| \hat{a}^\dagger \hat{a} \right| n \right\rangle \right) = \frac{1}{4} (2n+1) . \tag{39}$$

Similarly, one can obtain

$$\left\langle n \left| \hat{X}_2^2 \right| n \right\rangle = \frac{1}{4} (2n+1) . \tag{40}$$

Thus, the variances of quadratures are

$$\left\langle \left(\Delta \hat{X}_1 \right)^2 \right\rangle = \left\langle \left(\Delta \hat{X}_2 \right)^2 \right\rangle = \frac{1}{4} (2n+1) . \tag{41}$$

For $n \gg 1$, as it follows from (33) and (41), the variance product grows as n^2.

Since the Fock state is an eigenstate of photon number operator $\hat{n}$ (see (17)), the variance of photon number is equal to

$$\left\langle (\Delta \hat{n})^2 \right\rangle = 0. \tag{42}$$

Eq. (42) implies a non-fluctuating photon number in the beam of quantized light at each moment of time. Hence, the Fock states are usually referred to *photon number states*.

2.4 Optical coherent states

Lasers play an important role in science, information and communication, industry, medicine, ecology, etc. Although lasers are sometimes regarded as a classical source of the e.m. field, it is not correct in a general case. Quantum fluctuations are crucial in laser field characteristics and may be explored in different scientific applications of quantum technologies and photonics. Here, we represent a simple quantum optical description of single mode laser radiation well above the threshold. It is based on the famous Glauber approach to coherent states in optics.

We introduce coherent state $|\alpha\rangle$ as an eigenstate of photon annihilation operator $\hat{a}$, as follows

$$\hat{a}\,|\alpha\rangle = \alpha\,|\alpha\rangle\,, \tag{43}$$

where α is a complex number, eigenvalue of $\hat{a}$. Notably, the Hermitian conjugate of (43) equation reads as

$$\langle\alpha|\,\hat{a}^{\dagger} = \langle\alpha|\,\alpha^{*}. \tag{44}$$

We can search for the solution of Eqs. (43) and (44) as a linear superposition of infinite number of Fock states $|n\rangle$. After some straightforward calculations the solution of Eq. (43) may be found in the form

$$|\alpha\rangle = \exp\left(-\frac{1}{2}\,|\alpha|^{2}\right)\sum_{n=0}^{\infty}\frac{\alpha^{n}}{(n!)^{1/2}}\,|n\rangle\,. \tag{45}$$

It is easy to verify normalization condition for $|\alpha\rangle$ as

$$\langle\alpha|\alpha\rangle = e^{-|\alpha|^{2}}\sum_{n=0}^{\infty}\frac{|\alpha|^{2n}}{n!} = e^{-|\alpha|^{2}}e^{+|\alpha|^{2}} = 1. \tag{46}$$

Noteworthy, two arbitrary coherent states $|\alpha\rangle$, $|\beta\rangle$ are not orthogonal. It is possible to prove that

$$|\langle\alpha|\beta\rangle|^{2} = \exp\left(-\,|\alpha-\beta|^{2}\right). \tag{47}$$

Thus, the coherent states form an overcomplete set of states in the Hilbert space. However, for large enough amplitudes $\alpha \neq \beta$, it is possible to assume that overlapping of coherent states $|\langle\alpha|\beta\rangle|^{2}$ goes to zero.

Let us consider statistical properties of the single-mode field in coherent state $|\alpha\rangle$. The expected values of photon annihilation and creation operators, $\langle\alpha\,|\hat{a}|\,\alpha\rangle$, are immediately obtained with the right and left eigenvalue properties (43), (44),

$$\langle\hat{a}\rangle \equiv \langle\alpha\,|\hat{a}|\,\alpha\rangle = \alpha, \quad \left\langle\hat{a}^{\dagger}\right\rangle \equiv \left\langle\alpha\,\middle|\hat{a}^{\dagger}\middle|\,\alpha\right\rangle = \alpha^{*}. \tag{48}$$

From (48) the physical meaning of α becomes clear. For an average value of electric field operator $\hat{\mathbf{E}}\,(\mathbf{r},t)$ defined in (18), we obtain

$$\left\langle\alpha\,\middle|\hat{\mathbf{E}}\,(\mathbf{r},t)\middle|\,\alpha\right\rangle = i\left(\frac{\hbar\omega}{2\varepsilon_{0}V}\right)^{\frac{1}{2}}\mathbf{e}_{x}\left[\alpha e^{i(\mathbf{kr}-\omega t)} - \alpha^{*}e^{-i(\mathbf{kr}-\omega t)}\right]. \tag{49}$$

Since the e.m. field in (49) is polarized in the X direction, for simplicity we examine its scalar component. Establishing α in the polar form, $\alpha = |\alpha| e^{i\phi}$, from (49) we obtain

$$\left\langle \alpha \left| \hat{E}(\mathbf{r},t) \right| \alpha \right\rangle = 2|\alpha| \left(\frac{\hbar\omega}{2\varepsilon_0 V} \right)^{\frac{1}{2}} \sin[\omega t - \mathbf{kr} - \phi]. \tag{50}$$

Eqs. (50) looks like a classical plane-wave monochromatic field with amplitude $\mathcal{E}$, that is (cf. [6])

$$\mathrm{E}(t) = \frac{1}{2}\left(\mathcal{E} e^{i(\omega t - \mathbf{kr})} + \mathcal{E}^* e^{-i[\omega t - \mathbf{kr}]}\right) = |\mathcal{E}| \cos[\omega t - \mathbf{kr} - \theta], \tag{51}$$

where θ is the phase of classical field.

These simple arguments hint us to consider the correspondence between classical field amplitude $\mathcal{E}$ and parameter α in the form

$$\mathcal{E} \mapsto 2i \left(\frac{\hbar\omega}{2\varepsilon_0 V} \right)^{\frac{1}{2}} \alpha, \quad \mathcal{E}^* \mapsto -2i \left(\frac{\hbar\omega}{2\varepsilon_0 V} \right)^{\frac{1}{2}} \alpha^*. \tag{52}$$

Average photon number $\langle \alpha | \hat{n} | \alpha \rangle$ is immediately obtained using (43) and (44) as

$$\langle \hat{n} \rangle = \left\langle \alpha \left| \hat{a}^\dagger \hat{a} \right| \alpha \right\rangle = \langle \alpha | \alpha^* \cdot \alpha | \alpha \rangle = |\alpha|^2 . \tag{53}$$

Thus, real parameter $|\alpha|$ plays the role of classical field amplitude for the coherent light field.

Now we are ready to consider the fluctuations of e.m. radiation in the coherent state. The second moment of photon number may be calculated by the familiar normal ordering procedure, when all creation operators are moved to the left of the annihilation operators. This procedure uses commutation relation (6) and leads to

$$\hat{n}^2 = \hat{a}^\dagger \hat{a} \hat{a}^\dagger \hat{a} = \hat{a}^\dagger \left(\hat{a}^\dagger \hat{a} + 1 \right) \hat{a} = \hat{a}^\dagger \hat{a}^\dagger \hat{a} \hat{a} + \hat{a}^\dagger \hat{a}. \tag{54}$$

We can easily evaluate mean values of the normally-ordered operator in the form (54) for the coherent state using (43), (44). Thus, from (54) we obtain

$$\left\langle \hat{n}^2 \right\rangle \equiv \left\langle \alpha \left| \hat{n}^2 \right| \alpha \right\rangle = |\alpha|^4 + |\alpha|^2 = \langle \hat{n} \rangle^2 + \langle \hat{n} \rangle . \tag{55}$$

Eq. (55) implies photon-number variance

$$\sigma_n^2 \equiv \left\langle (\Delta \hat{n})^2 \right\rangle = \langle \hat{n} \rangle = |\alpha|^2 . \tag{56}$$

Non-vanishing right-hand side of (56) is a consequence of photon statistical features in a coherent light beam. In quantum optics these features are inherent to the Poisson distribution for some n variable. Actually, the probability of finding n photons in single-mode coherent state $|\alpha\rangle$ may be obtained from definition (45) as

$$p_n = |\langle n|\alpha\rangle|^2 = \frac{|\alpha|^{2n}}{n!}e^{-|\alpha|^2} = \frac{\langle\hat{n}\rangle^n}{n!}e^{-\langle\hat{n}\rangle}, \tag{57}$$

which is obviously the Poisson probability distribution.

The relative (normalized) standard deviation of the photon number in coherent state is

$$\frac{\sigma_n}{\langle\hat{n}\rangle} = \frac{1}{|\alpha|} = \frac{1}{\sqrt{\langle\hat{n}\rangle}}. \tag{58}$$

In quantum theory photon number operator $\hat{n}$ represents a phase conjugate (non-commuting) variable to the phase of e.m. field. Correct definition of the phase operator is not a trivial task in quantum optics, see e.g. [3]. For a large enough mean photon number, the Heisenberg uncertainty relation for the particle number and phase implies (cf. [4])

$$\sigma_n^2\sigma_\phi^2 \geq \frac{1}{4}, \tag{59}$$

where σ_ϕ^2 defines a quantum phase variation. For coherent light we can put (56) in (59) and obtain

$$\sigma_\phi^2 = \frac{1}{4\,\langle\hat{n}\rangle}. \tag{60}$$

Physical scaling of the phase fluctuations reproduced in Eq. (60) plays an important role especially in quantum metrology. In particular, quantum measurement and subsequent estimation of some unknown relative phase parameter ϕ accumulated in Mach-Zehnder or Michelson interferometers may be performed by means of the input coherent probe field with the accuracy determined by $\sigma_{\phi,SQL} \simeq 1/\sqrt{\langle\hat{n}\rangle}$, which is known as the ***standard quantum limit*** of phase measurement, see e.g. [7]; σ_ϕ vanishes with an increasing average photon number in coherent state. For very large average photon number, $\langle\hat{n}\rangle \gg 1$, σ_ϕ goes to zero that means a well-defined phase of the field in coherent state.

Thus, Eqs. (50), (52) and (60) imply that coherent state is close to the classical one for very large field amplitude α.

We can obtain fluctuations of quadrature operators in coherent state by means of Eqs. (6), (30a), (30b), (44) and (45). After some algebra we arrive to

$$\left\langle \left(\Delta \hat{X}_1\right)^2 \right\rangle_\alpha = \left\langle \left(\Delta \hat{X}_2\right)^2 \right\rangle_\alpha = \frac{1}{4}. \tag{61}$$

Eq. (61) plays important role in quantum physics. It demonstrates that field quadrature variances in coherent state are the same as in vacuum one, cf. (36). Apparently, an arbitrary coherent state minimizes Heisenberg uncertainty relation (33).

Eq. (61) can help to elucidate fluctuations in single-mode electric field $\hat{E}\,(\mathbf{r},t)$. Standard deviation σ_E is

$$\sigma_E \equiv \left\langle \left(\Delta \hat{E}\right)^2 \right\rangle^{\frac{1}{2}} = \left(\frac{\hbar\omega}{2\varepsilon_0 V}\right)^{\frac{1}{2}}, \tag{62}$$

which is identical to the one for a vacuum state.

Some algebraic treatments can help to represent coherent state (45) in a more compact and mathematically appropriate form. In particular, by means of (34) we can rewrite definition (45) of the coherent state as

$$|\alpha\rangle = e^{-|\alpha|^2/2} \sum_{n=0}^{\infty} \frac{\left(\alpha \hat{a}^\dagger\right)^n}{n!} |0\rangle = \exp\left(\alpha \hat{a}^\dagger - \frac{1}{2}|\alpha|^2\right)|0\rangle\,. \tag{63}$$

Using vacuum state properties we can recast (63) as

$$|\alpha\rangle = \hat{D}\,(\alpha)\,|0\rangle\,, \tag{64}$$

where we introduce ***coherent-state displacement operator*** $\hat{D}\,(\alpha)$, defined as

$$\hat{D}\,(\alpha) = \exp\left(\alpha \hat{a}^\dagger - \alpha^* \hat{a}\right). \tag{65}$$

Thus, in agreement with Eq. (64), we can mathematically obtain coherent state by applying displacement operator $\hat{D}(\alpha)$ to the vacuum. Operator $\hat{D}(\alpha)$ satisfies the conditions

$$\hat{D}^\dagger\,(\alpha)\,\hat{D}\,(\alpha) = \hat{D}\,(\alpha)\,\hat{D}^\dagger\,(\alpha) = 1. \tag{66}$$

Eqs. (63) - (66) are typically used for elucidating various properties of the quantized e.m. field in schemes with non-classical light. These properties are beyond the scope of this course and may be found in a number of textbooks

on quantum optics, see e.g. [2, 3, 8]. Here, we only mention quasiprobability (Husimi) Q-function that for arbitrary pure state $|\psi\rangle$ may be defined as

$$Q = \frac{1}{\pi} |\langle \alpha|\psi\rangle|^2. \tag{67}$$

In quantum mechanics the joint probability function does not exist in phase space for the momentum and position (or Hermitian quadratures) because of uncertainty relation (2) between them. However, the quasiprobability function sometimes provides a fruitful information about given quantum state $|\psi\rangle$ of the system. For example, for arbitrary coherent state $|\psi\rangle = |\beta\rangle$ the Q - function is Gaussian and reproduces the result obtained in (47).

We summarize the obtained results in Fig. 3. Since two quadratures X_1 and X_2 of the e.m. field are relevant to the position and momentum of the quantum optical oscillator, it is helpful to establish an arbitrary state of light in the X_1 – X_2 phase plane.

In *classical* electrodynamics the state of ideal (non-fluctuating) e.m. field may be represented by a dot in a phase space (it is A in Fig. 3(a)). Within classical approach, e.m. field possesses well – defined amplitude and phase, which are established by ϕ, x_1, and x_2 variables in Fig. 3(a), respectively.

In *quantum* domain, because of uncertainty relation (33), the state of quantum field in phase plane occupies some region, which is inherent to quantum fluctuations of field quadtratures, amplitude (photon number), and phase, respectively. The field circle in Fig. 3(b) is relevant to *vacuum state* of light and demonstrates quantum fluctuations possessing zero averages for both quadratures.

The *coherent state* of light is described by the same quadrature variances but shifted from the zero point by field amplitude $|\alpha|$, Fig. 3(c). The fluctuations of the field quadrature variables are the same as for vacuum. The state approaches to the classical one possessing well-defined phase by increasing the mean photon number (field amplitude).

Schematically, statistical features of photonic field quadratures in the *Fock state* is outlined in Fig. 3(d). Since the photon number variance is zero (see (17)), we deal here with a circle-like uncertainty, which fixes the field amplitude (photon number n) leaving phase ϕ undefined. Loosely speaking, the Fock state is a limiting state of the e.m. field, which requires maintenance of well-defined photonic energy throughout the whole measurement procedure. Therefore, creation of the Fock state with a *large number* of photons represents a difficult task

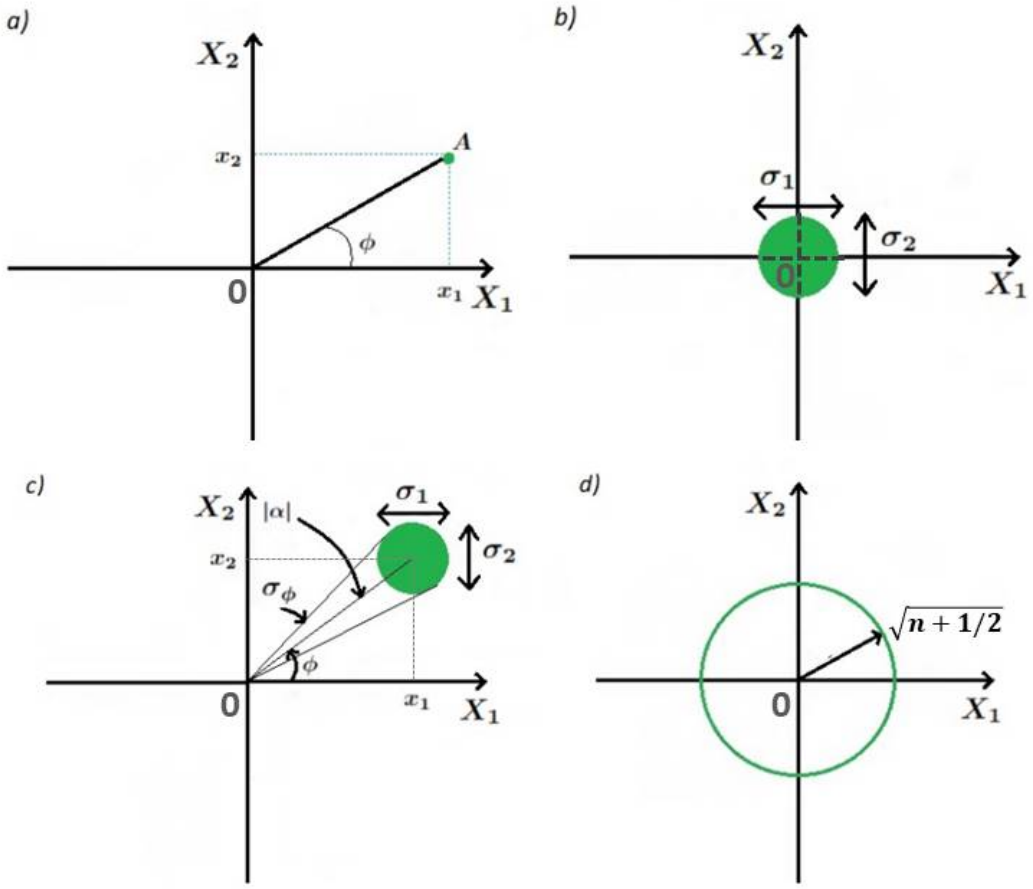

Fig. 3: Phase-space portrait of a) classical, b) vacuum, c) coherent, and d) Fock states of light. The $x_{1,2}$ are average values of quadratures. Field regions characterize standard deviations $\sigma_{1,2} = \langle(\Delta\hat{X}_{1,2})^2\rangle^{1/2} = 1/2$ of quadratures for vacuum and coherent states, respectively

in real-world experiments.

2.5 Problems

1. Prove that the energy of classical e.m. field in the cavity with volume V may be established as (cf. Fig. 1)

$$E_F = \frac{1}{2}\left(\epsilon_0 \mathrm{E}^2 + \frac{\mathrm{B}^2}{\mu_0}\right) = \frac{V}{4}\left(\epsilon_0 \mathcal{E}^2 \sin^2[\omega t] + \frac{\mathcal{B}^2}{\mu_0}\cos^2[\omega t]\right). \tag{68}$$

2. Prove that Eq. (68) corresponds to the classical electromagnetic harmonic oscillator in form

$$x(t) = \sqrt{\frac{\epsilon_0 V}{2\omega^2}}\,\mathcal{E}\,\sin[\omega t], \tag{69a}$$

$$p(t) = \sqrt{\frac{V}{2\mu_0}}\,\mathcal{B}\,\cos[\omega t] = \sqrt{\frac{\epsilon_0 V}{2}}\,\mathcal{E}\,\cos[\omega t]. \tag{69b}$$

3. Prove that momentum operator $\hat{p} = -i\hbar\frac{d}{dx}$ of the quantum harmonic oscillator is Hermitian.

4. Check commutation relation (1) for the quantum harmonic oscillator accounting definition of position $\hat{x}$ and momentum $\hat{p}$ operators in quantum mechanics.

5. Check commutation relation in (32).

6. Prove that photon number operator $\hat{n}$ defined in (9) is Hermitian.

7. Give a matrix form for photon number operator (9).

8. Prove Eq. (34).

9. Derive Eq. (35).

10. Check that coherent state (45) represents a solution of Eqs. (43), (44).

11. Prove commutation relations

$$\left[\hat{a},\ \left(\hat{a}^\dagger\right)^2\right] = 2\hat{a}^\dagger, \quad \left[\hat{a}^2,\ \hat{a}^\dagger\right] = 2\hat{a}. \tag{70}$$

12. Prove commutation relations

$$\left[\hat{a},\ \left(\hat{a}^\dagger\right)^n\right] = n\left(\hat{a}^\dagger\right)^{n-1}; \quad \left[\hat{a}^n,\ \hat{a}^\dagger\right] = n\hat{a}^{n-1}, \tag{71}$$

where n is a positive integer.

13. Prove Eq. (47).

14. Prove

$$\left[\hat{a},\, \exp\left(\beta\hat{a}^{\dagger}\right)\right] = \beta \exp\left(\beta\hat{a}^{\dagger}\right), \tag{72}$$

where operator $\exp\left(\beta\hat{a}^{\dagger}\right)$ is defined by its Maclaurin series of powers of $\beta\hat{a}^{\dagger}$.

15. Prove the Baker-Hausdorf formula for any two operators $\hat{A}$ and $\hat{B}$,

$$e^{i\lambda\hat{A}}\hat{B}e^{-i\lambda\hat{A}} = \hat{B} + i\lambda\left[\hat{A},\hat{B}\right] + \frac{(i\lambda)^2}{2!}\left[\hat{A},\left[\hat{A},\hat{B}\right]\right] + ... \tag{73}$$

16. For two operators $\hat{A}$ and $\hat{B}$, which satisfy conditions $\left[\hat{A},\hat{B}\right] \neq 0$ and $\left[\hat{A},\left[\hat{A},\hat{B}\right]\right] = 0 = \left[\hat{B},\left[\hat{A},\hat{B}\right]\right]$, prove the Baker-Hausdorf-Campbell theorem

$$e^{\hat{A}+\hat{B}} = e^{-\frac{1}{2}\left[\hat{A},\hat{B}\right]}e^{\hat{A}}e^{\hat{B}} = e^{\frac{1}{2}\left[\hat{A},\hat{B}\right]}e^{\hat{B}}e^{\hat{A}}. \tag{74}$$

17. Derive Eq. (64).

18. Calculate average photon number $\langle\hat{n}\rangle$ and photon number variance $\left\langle(\Delta\hat{n})^2\right\rangle$ in laser beam by means of Poisson probability distribution (57).

19. Consider the superposition of the vacuum and one-photon states that is called *qubit state* and may be defined as

$$|\psi\rangle = C_1|0\rangle + C_2|1\rangle, \tag{75}$$

where C_1 is real, and C_2 is a complex number.

1) Represent qubit state (75) in a matrix form.

2) Derive normalization condition $\langle\psi|\psi\rangle = 1$ for (75).

3) What is the physical meaning of C_1 and C_2 coefficients? Are they independent?

4) Consider qubit (75) as a limiting coherent state (45) with amplitude $|\alpha| \ll 1$. Recover C_1 and C_2 coefficients for this case.

5) Compute the average photon number for state in (75).

6) Compute the variance of photon number for state in (75).

7) Suppose that $C_2 = |C_2|e^{i\theta}$. What is the physical meaning of phase θ? How can we obtain θ experimentally?

20. Suppose that we have *two-qubit state*

$$|\Psi\rangle = |\psi_1\rangle \otimes |\psi_2\rangle, \tag{76}$$

where $|\psi_{1,2}\rangle$ is defined as

$$|\psi_1\rangle = \frac{1}{\sqrt{3}}|0\rangle - \sqrt{\frac{2}{3}}|1\rangle; \tag{77a}$$

$$|\psi_2\rangle = \frac{1}{\sqrt{2}}\left(|0\rangle + i\,|1\rangle\right). \tag{77b}$$

1) Prove that state $|\Psi\rangle$ is normalized to 1.

2) Find the matrix form for state $|\Psi\rangle$.

3) What is the probability to find two-qubit state $|\Psi\rangle$ as ground state $|0\rangle \otimes |0\rangle$?

21. Prove

$$\hat{D}^{\dagger}(\alpha)\,\hat{a}\hat{D}(\alpha) = \hat{a} + \alpha; \tag{78a}$$

$$\hat{D}^{\dagger}(\alpha)\,\hat{a}^{\dagger}\hat{D}(\alpha) = \hat{a}^{\dagger} + \alpha^{*}. \tag{78b}$$

22. Prove that for large photon number $\langle\hat{n}\rangle$ Poisson distribution (57) may be replaced by Gaussian distribution function

$$P(n) = \frac{1}{\sqrt{2\pi\,\langle\hat{n}\rangle}}\exp\left\{-\frac{(n-\langle\hat{n}\rangle)^2}{2\,\langle\hat{n}\rangle}\right\}. \tag{79}$$

23. Calculate Q-function for Fock state $|\psi\rangle = |n\rangle$ and plot it for different n.

24. Consider macroscopic superposition of two coherent states $|\alpha\rangle$, $|\beta\rangle$, which are two distinct eigenstates of photon annihilation operator $\hat{a}$, cf. (43). Let us represent this superposition as

$$|\Upsilon\rangle = \mathcal{N}\left(|\alpha\rangle + e^{i\varphi}\,|\beta\rangle\right), \tag{80}$$

where $\mathcal{N}$ is a normalization constant, φ is an arbitrary phase. Find normalization constant $\mathcal{N}$ in (80).

25. In literature, state (80) with $\beta = -\alpha$ is referred as a ***Schrödinger cat state***, cf. [5].

1) Prove that two states obtained from (80) with $\beta = -\alpha$, $\varphi = 0$ and $\varphi = \pi$ represent even and odd Schrödinger-cat states in respect of photon number n.

2) Find mean values of quadratures $\langle\Upsilon|\hat{X}_1|\Upsilon\rangle$, $\langle\Upsilon|\hat{X}_2|\Upsilon\rangle$.

3) Compute average photon number $\langle \Upsilon|\hat{n}|\Upsilon\rangle$.

4) Find variances of Hermitian quadratures $\left\langle (\Delta \hat{X}_{1,2})^2 \right\rangle_{\Upsilon}$ in state (80) and represent them schematically on the phase plane as in Fig. 3. Examine uncertainty relation (33) for the results obtained.

5) Calculate variance of the photon number $\left\langle (\Delta \hat{n})^2 \right\rangle_{\Upsilon}$. Compare the result obtained with variance (56) for an ordinary coherent state.

6) Calculate Q-function for Schrödinger-cat state and plot it.

7) Depict Schrödinger-cat state in phase space as it is done in Fig. 3.

3 Interaction of Quantum Two-Level System With Classical Laser Field

Here, we establish the coherent matter – light interaction problem in the semiclassical limit and for ideal two-level systems, i.e. neglecting various broadening mechanisms of spectral lines, cf. [8].

3.1 General description of interaction of quantum two-level system with classical field

In many applications of quantum science the simplest quantum ***two-level system (TLS)*** plays a central role. Although the whole system may be complex enough, in some cases it is possible to find energy levels well-distinguished in experiment; these levels are ground ($|g\rangle$) and excited ($|e\rangle$) states, see Fig. 4. Notably, TLS may be designed by means of so-called artificial atoms – quantum dots, superconductor circuits, etc. States $|e\rangle$ and $|g\rangle$ can be represented in as vectors:

$$|g\rangle = \begin{pmatrix} 0 \\ 1 \end{pmatrix}, \quad |e\rangle = \begin{pmatrix} 1 \\ 0 \end{pmatrix}, \tag{81}$$

where $|e\rangle$ and $|g\rangle$ form an orthonormal basis in the Hilbert space:

$$\langle g|g\rangle = \langle e|e\rangle = 1, \quad \langle g|e\rangle = \langle e|g\rangle = 0. \tag{82}$$

We assume that $E_g = \hbar\omega_g$ and $E_e = \hbar\omega_e > E_g$ are two experimentally

distinguishable eigenenergies of TLS Hamiltonian $\hat{H}_{TLS}$:

$$\hat{H}_{TLS}\,|e\rangle = \hbar\omega_e\,|e\rangle\,; \tag{83a}$$

$$\hat{H}_{TLS}\,|g\rangle = \hbar\omega_g\,|g\rangle\,, \tag{83b}$$

where H_{TLS} is given in the form

$$\hat{H}_{TLS} = \hbar\omega_g\,|g\rangle\,\langle g| + \hbar\omega_e\,|e\rangle\,\langle e| = \begin{pmatrix} \hbar\omega_e & 0 \\ 0 & \hbar\omega_g \end{pmatrix}. \tag{84}$$

Here, we suppose that $\hat{H}_{TLS}$ is time-independent. We denote the corresponding frequency of transition $|g\rangle \leftrightarrow |e\rangle$ as $\omega_0 \equiv \omega_e - \omega_g$, see Fig. 4.

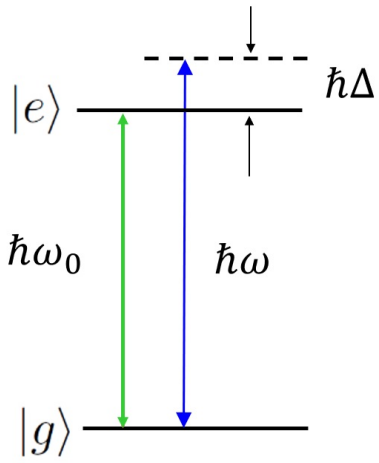

Fig. 4: Schematic representation of energy levels for TLS interacting with driving field of angular frequency ω. The resonant angular frequency between energy levels is ω_0; $\Delta = \omega - \omega_0$ is the detuning. For many important applications one can assume that the detuning admits the modest values of Δ and inequalities $|\Delta| \ll \omega_0$, ω are satisfied

Let TLS interact with the classical monochromatic light beam within dipole approximation (28), which possesses electric field in the form (cf. (51))

$$\mathrm{E}\,(t) = \frac{1}{2}\big(\mathcal{E}e^{i\omega t} + \mathcal{E}^* e^{-i\omega t}\big) = |\mathcal{E}|\cos\,(\omega t - \theta), \tag{85}$$

where $\mathcal{E}$, ω, and θ are field amplitude, angular frequency, and phase, respectively. Then, we can examine the case of real field amplitude $\mathcal{E}$ that is valid for $\theta = 0$. In (85) we omit polarization assuming that TLS eigenstates fulfil some selection rules.

We take the Hamiltonian of TLS interacted with the e.m. classical field as

$$\hat{H} = \hat{H}_{TLS} + \hat{H}_I(t), \tag{86}$$

where $\hat{H}_I(t)$ is part of the total Hamiltonian responsible for interaction. In the dipole approximation we can assume that (cf. [8])

$$\hat{H}_I(t) = -\big(\wp_{ge} |g\rangle \langle e| + \wp_{eg} |e\rangle \langle g| \big) E(t), \tag{87}$$

where $\wp_{ge} = \wp^*_{eg}$ is non-zero dipole matrix element.

Exploring definitions (81) we recast Eq. (87) in the matrix form as

$$\hat{H}_I = -\mathcal{E} \cos(\omega t) \begin{pmatrix} 0 & \wp_{eg} \\ \wp^*_{eg} & 0 \end{pmatrix}. \tag{88}$$

Further we suppose that $\wp_{eg}$ is real.

Combining (84) and (88) for total Hamiltonian $\hat{H}$ represented it in the matrix form we obtain

$$\hat{H} = \hbar \begin{pmatrix} \omega_e & -\Omega_R \cos(\omega t) \\ -\Omega_R \cos(\omega t) & \omega_g \end{pmatrix}, \tag{89}$$

where we have introduced Rabi frequency

$$\Omega_R = \frac{\wp_{eg} \mathcal{E}}{\hbar} \tag{90}$$

that completely characterizes matter-field interaction features.

3.2 Rabi oscillations

Our approach presumes the solution of Schrödinger equation

$$i\hbar \frac{\mathrm{d} |\Psi\rangle}{\mathrm{d}t} = \hat{H} |\Psi\rangle, \tag{91}$$

where $|\Psi\rangle$ is a quantum state of TLS that we establish as

$$|\Psi\rangle = C_e(t) |e\rangle + C_g(t) |g\rangle = \begin{pmatrix} C_e(t) \\ C_g(t) \end{pmatrix}. \tag{92}$$

In (92) $C_e(t)$ and $C_g(t)$ are time-dependent probability amplitudes, which obey

$$|C_e(t)|^2 + |C_g(t)|^2 = 1 \tag{93}$$

normalization condition. $P_e(t) = |C_e(t)|^2$ is the probability to find TLS in the excited state.

Thus, even if TLS is initially in a ground state, which means $C_g(0) = 1$, and $C_e(0) = 0$, then, after some time it transfers to superposition state (92). Thus, the TLS state is unknown until the energy is measured. Then, with some probabilities we find that TLS is in either the ground or excited state.

Now we should solve Schrödinger equation (91) with Hamiltonian (89) and find $C_{e,g}$ complex functions. Substituting (92) into (91) with (89) we obtain a set of equations

$$\begin{pmatrix} i\dot{C}_e \\ i\dot{C}_g \end{pmatrix} = \begin{pmatrix} \omega_e & -\Omega_R \cos(\omega t) \\ -\Omega_R \cos(\omega t) & \omega_g \end{pmatrix} \begin{pmatrix} C_e \\ C_g \end{pmatrix}, \tag{94}$$

where dots denote derivatives with respect to time.

The free parts of Eqs. (94) may be eliminated if we introduce new variables F_e, F_g as follows

$$F_e = C_e e^{i\omega_e t}, \quad F_g = C_g e^{i\omega_g t}. \tag{95}$$

The obtained equations have a form

$$\dot{F}_g = i\Omega_R \cos(\omega t) e^{-i\omega_0 t} F_e; \tag{96a}$$

$$\dot{F}_e = i\Omega_R \cos(\omega t) e^{i\omega_0 t} F_g. \tag{96b}$$

In ***rotating wave approximation (RWA)*** we suppose that terms containing exponents with $\omega + \omega_0$ oscillate rapidly in comparison with terms with detuning rate $\Delta \equiv \omega - \omega_0$, i.e. we assume $\Delta \ll \omega + \omega_0$. In this limit Eqs. (96) approach to

$$\dot{F}_g = i\frac{\Omega_R}{2} e^{i\Delta t} F_e; \tag{97a}$$

$$\dot{F}_e = i\frac{\Omega_R}{2} e^{-i\Delta t} F_g. \tag{97b}$$

Eqs. (97) admit periodic solutions. They look very simple if we put detuning $\Delta = 0$. Suppose that TLS is initially placed in the ground state (at $t = 0$), i.e. we have $F_g(0) = 1$ and $F_e(0) = 0$. Then, we obtain

$$F_e(t) = i \sin(\Omega_R t/2); \tag{98a}$$

$$F_g(t) = \cos(\Omega_R t/2). \tag{98b}$$

The probability of the TLS to be in the excited state is

$$P_e(t) \equiv |C_e|^2 = |F_e|^2 = \sin^2(\Omega_R t/2). \tag{99}$$

For short time periods or weak e.m. field when $\Omega_R t \ll 1$, from (99) one can obtain

$$P_e(t) \simeq \frac{1}{4}\Omega_R^2 t^2, \tag{100}$$

which manifests the increasing of excitation probability in time as t^2. The population inversion is

$$W \equiv P_e - P_g = -\cos(\Omega_R t). \tag{101}$$

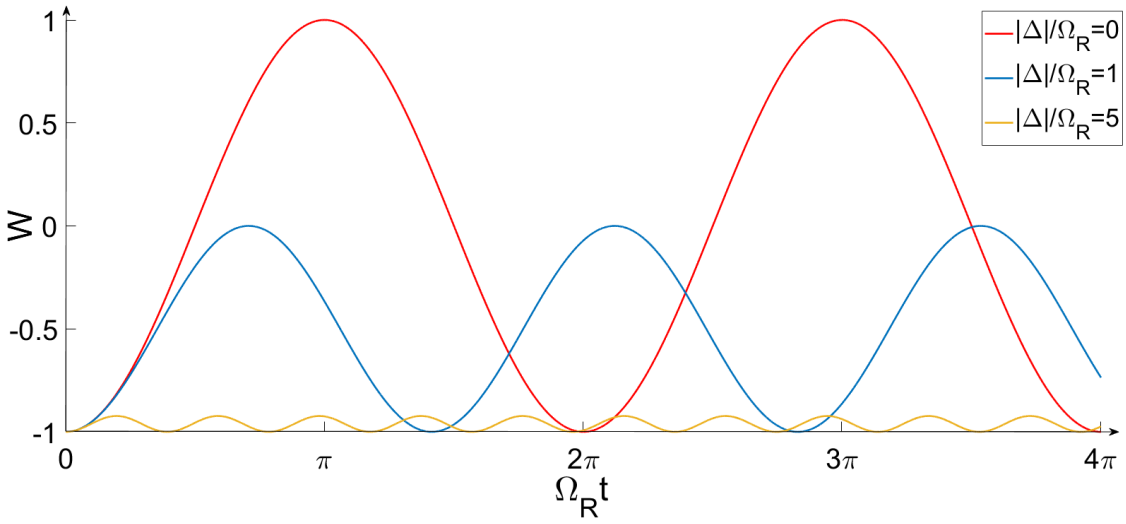

Fig. 5: Temporal dependence of population imbalance W of TLS interacting with classical e.m. field without losses and decoherence in general

Thus, Eq. (101) implies periodic Rabi oscillations for the population inversion for a given TLS. Such oscillatory features in response to the strong (classical) light field are called ***Rabi oscillations*** or ***Rabi flopping***. The amplitude of oscillation is maximal for detuning in the vicinity of resonance $\Delta = 0$.

The coherence of TLS interaction with e.m. field is described by TLS polarization that may be determined as

$$\begin{aligned} \mathrm{P} \equiv \wp_{eg}[C_e^* C_g + C_g^* C_e] &= \wp_{eg}[F_e^* F_g e^{i\omega_0 t} + F_g^* F_e e^{-i\omega_0 t}] \\ &= \wp_{eg} \sin(\Omega_R t) \sin(\omega_0 t). \end{aligned} \tag{102}$$

Notice, the P and W variables are shifted by $\pi/2$.

3.3 Dressed states

In quantum optics there exist so-called dressed states, which represent an important physical solution of matter-wave interaction, see e.g. [9]. In quantum domain, dressed state solutions can be obtained in different ways, when the cavity field is strong enough. Let us make a time-dependent transformation in Eqs. (97):

$$c_g(t) = C_g(t); \tag{103a}$$

$$c_e(t) = C_e(t) e^{-i\Delta t}. \tag{103b}$$

New variables $c_{e,g}$ satisfy the equations, which we represent in the matrix form

$$\begin{pmatrix} \dot{c}_e \\ \dot{c}_g \end{pmatrix} = -\frac{i}{\hbar} \begin{pmatrix} -\hbar\Delta & \hbar\Omega_R/2 \\ \hbar\Omega_R/2 & 0 \end{pmatrix} \begin{pmatrix} c_e \\ c_g \end{pmatrix}. \tag{104}$$

Matrix

$$H' = \begin{pmatrix} -\hbar\Delta & \hbar\Omega_R/2 \\ \hbar\Omega_R/2 & 0 \end{pmatrix} \tag{105}$$

represents our new time-independent Hamiltonian that admits eigenenergies $E_{1,2}$ and (unnormalized) eigenstates $|\pm\rangle$ in the form

$$E_{1,2} = \frac{\hbar}{2}(-\Delta \pm \omega_R); \tag{106}$$

$$|+\rangle = \begin{pmatrix} \omega_R - \Delta \\ \Omega_R \end{pmatrix}; \tag{107a}$$

$$|-\rangle = \begin{pmatrix} \omega_R + \Delta \\ -\Omega_R \end{pmatrix}, \tag{107b}$$

where ω_R is full Rabi splitting (angular) frequency, which is determined as

$$\omega_R = \sqrt{\Omega_R^2 + \Delta^2}. \tag{108}$$

Now we can recast states $|\pm\rangle$ as

$$|+\rangle = \cos(\Theta/2)\,|e\rangle + \sin(\Theta/2)\,|g\rangle\,; \tag{109a}$$

$$|-\rangle = -\sin(\Theta/2)\,|e\rangle + \cos(\Theta/2)\,|g\rangle\,, \tag{109b}$$

where we define

$$\tan(\Theta) = -\frac{\Omega_R}{\Delta}. \tag{110}$$

In (110) Θ angle lies $0 \leq \Theta < \pi$.

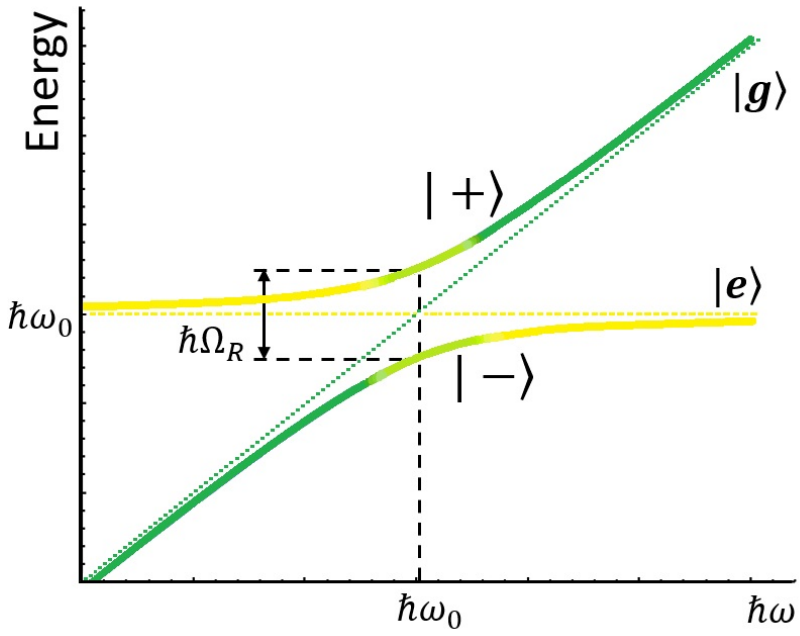

Fig. 6: Energies of coupled TLS – light dressed states levels against $\hbar\omega$. The dashed lines correspond to the uncoupled (bare) states; $\hbar\Omega_R$ is the resonant Rabi splitting energy

The states, determined by Eqs. (109)- (110) are ***dressed states***. They are often used to describe Rabi splitting phenomena and to explain obtained spectral features.

Fig. 6 schematically demonstrates the dependence of dressed TLS state energies versus photonic energy $\hbar\omega$. The energies of the dressed state levels create

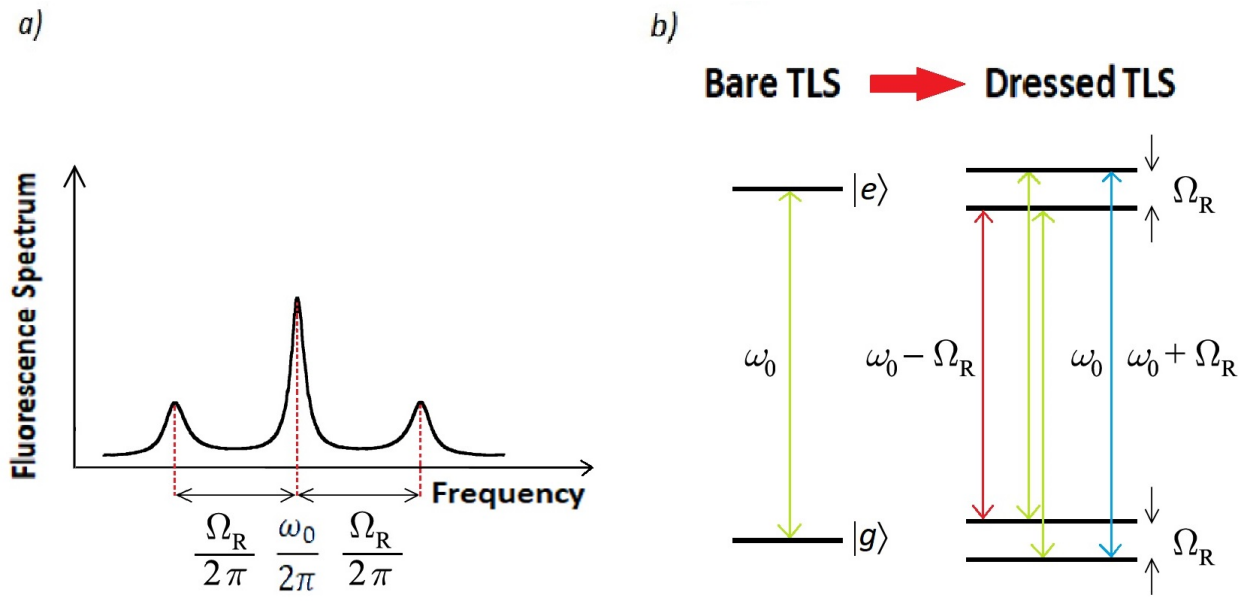

Fig. 7: a) Schematic fluorescence spectrum (Mollow triplet) in the presence of two-level atom – light resonant interaction. b) Energy (population) transfer between levels of different manifolds given in dressed state representation. The color lines correspond to Mollow triplet (spectral) components

two branches of a hyperbola. The minimal frequency gap between dressed states is Rabi splitting frequency Ω_R that occurs in the vicinity of resonance condition $\Delta = 0$. State $|+\rangle$ is always placed above state $|-\rangle$. At $\Delta \neq 0$ $|+\rangle$ and $|-\rangle$ repel each other and demonstrate so-called, anti-crossing effect.

The dressed states representation allows to describe the fluorescence spectrum presented in Fig. 7(a). In 1969, Mollow firstly discussed that the fluorescence spectrum may split into a triplet with the components possessing angular frequencies of ω_0 and $\omega_0 \pm \Omega_R$. In the experiment one can obtain spectral peaks at ω_0 and at sidebands at $\omega_0 \pm \Omega_R$. The occurrence of these peaks are easily explained in Fig. 7(b) by dressed states. In particular, angular frequencies of allowed transition represent a population transfer between energy levels. It is important to note that transitions between dressed states with photon emission are prohibited.

3.4 Problems

1. What is a selection rule? Give examples.

2. How do linear and circular polarizations of the e.m. field affect H_I matrix elements? Consider hydrogen-like atom.

4. Solve Eqs. (97a), (97b) assuming that TLS is initially in the excited state.

5. Solve Eqs. (97a), (97b) for $\Delta \neq 0$ by the Laplace transform method.

6. Solving Eqs. (97a), (97b) prove that for non-zero detuning $\Delta \neq 0$ Rabi frequency ω_R takes the form (108).

7. Examine and plot probability P_e of TLS excitation in the limit of $\Delta^2 \gg \Omega_R^2$.

8. How can you explain physically that TLS polarization and population imbalance are shifted by $\pi/2$?

9. Consider interaction of light field with hydrogen atom possessing resonant 1s $\rightarrow$ 2p transition at 137 nm (atomic dipole is $0.74ea_0 = 6.32 \times 10^{30}$ C$\cdot$ m. Calculate period $T_R = 2\pi/\Omega_R$ of Rabi oscillations for optical intensity $10\text{kW}/m^2$, cf. [2].

Answer: $T_R = 38$ ns.

Hint: Consider the intensity of light field that relates to its electric field amplitude as $I = \frac{1}{2}c\epsilon_0 n\mathcal{E}^2$, where n is the refractive index of the medium, $\epsilon_0 = 8.854 \times 10^{12}$ F/m is electric permittivity of free space taken in SI units, c is the speed of light in the vacuum.

10. Obtain Eqs. (106), (107).

11. Prove that dressed states (109) satisfy the normalization condition. Are they mutually orthogonal?

12. Prove that far from resonance energies (106) are

$$E_1 = E_g + \frac{\hbar\Omega_R^2}{4\Delta}; \tag{111a}$$

$$E_2 = E_e - \frac{\hbar\Omega_R^2}{4\Delta}. \tag{111b}$$

In particular, energy shifts quadratically depend on the driving field, which is

known as "light shifts" or AC-Stark shifts.

13. Consider Eqs. (109)- (110) in the limiting far-from-resonance case, when $|\Delta| \gg \Omega_R$. How do dressed states behave in this limit? Examine separately positive and negative detuning Δ.

4 Simple Quantum Models of Light-Matter Interaction

In quantum theory of matter-light interaction there are only few models, which are exactly solvable and fully quantum-mechanical. In this Section we consider some of them.

4.1 The Jaynes-Cummings model

The Jaynes-Cummings (JC) model represents a milestone in quantum theory of matter – field interaction. To obtain the JC model we should include quantization of the e.m. field into familiar semiclassical Hamiltonian (86) that describes the interaction between a TLS and a single mode e.m. field:

$$\hat{H} = \hat{H}_{TLS} + \hat{H}_F + \hat{H}_I(t). \tag{112}$$

Let us specify all the terms in (112) for the JC model. Term $\hat{H}_F$ in (112) represents the Hamiltonian of quantized free e.m. field, that is (cf. (8))

$$\hat{H}_F = \hbar\omega \hat{a}^\dagger \hat{a}. \tag{113}$$

As total quantum Hamiltonian (112) of matter – field interaction is usually specified up to the constant term, which gives some unimportant energy shift, we omit constant energy term $\hbar\omega/2$ in (113). In $\hat{H}_I(t)$ we can take into account quantized (linearly polarized) field if we consider field operator (29) in (87) instead of classical function $E(t)$. In the dipole approximation we suppose that

$$\hat{H}_I(t) = -\left(\wp_{ge} |g\rangle \langle e| + \wp_{eg} |e\rangle \langle g|\right) \hat{E}(t). \tag{114}$$

Inserting (29) into (114) we obtain

$$\hat{H}_I(t) = -i\hbar g(\hat{\sigma}_- + \hat{\sigma}_+) \left(\hat{a}e^{-i\omega t} - \hat{a}^\dagger e^{i\omega t}\right), \tag{115}$$

where

$$g \equiv \left(\frac{\omega}{2\hbar\varepsilon_0 V}\right)^{\frac{1}{2}} \wp_{ge} \tag{116}$$

is the strength of single TLS interaction with cavity quantum field; we assume that $\wp_{ge} = \wp_{eg}^*$ is real.

In (115) we also introduce the downward ($\hat{\sigma}_-$) and upward ($\hat{\sigma}_+ = \hat{\sigma}_-^\dagger$) transition operators as

$$\hat{\sigma}_+ \equiv |e\rangle\langle g|, \quad \hat{\sigma}_- \equiv |g\rangle\langle e|. \tag{117}$$

Taking into account (82) it is easy to verify the rules for operators (117) in the form

$$\hat{\sigma}_+ |e\rangle = 0, \quad \hat{\sigma}_+ |g\rangle = |e\rangle, \tag{118a}$$

$$\hat{\sigma}_- |e\rangle = |g\rangle, \quad \hat{\sigma}_- |g\rangle = 0. \tag{118b}$$

The operators (117) obey commutation relations

$$[\hat{\sigma}_+,\, \hat{\sigma}_-] = \hat{\sigma}_z, \quad [\hat{\sigma}_z,\, \hat{\sigma}_\pm] = \pm 2\hat{\sigma}_\pm, \tag{119}$$

where $\hat{\sigma}_z = |e\rangle\langle e| - |g\rangle\langle g|$ is an operator that describes TLS inversion.

Noteworthy, the photon annihilation, $\hat{a}$, and creation, $\hat{a}^\dagger$, operators commute with any sigma-operators $\hat{\sigma}_\pm, \hat{\sigma}_z$ inherent to TLS.

Moving from the Schrödinger picture to a so-called *interaction picture* we can assume in (115) that operators $\hat{\sigma}_\pm$ evolve in time as $\hat{\sigma}_\pm = \hat{\sigma}_\pm e^{\pm i\omega_0 t}$. Thus, one can rewrite Eq. (115) as

$$\begin{aligned} \hat{H}_I(t) = &-i\hbar g\left(\hat{\sigma}_-\hat{a}e^{-i(\omega+\omega_0)t} - \hat{\sigma}_+\hat{a}^\dagger e^{i(\omega+\omega_0)t}\right) - \\ &-i\hbar g\left(\hat{\sigma}_+\hat{a}e^{-i(\omega-\omega_0)t} - \hat{\sigma}_-\hat{a}^\dagger e^{i(\omega-\omega_0)t}\right). \end{aligned} \tag{120}$$

Rotating wave approximation (RWA) allows to omit the first bracket in (120). In this limiting case we obtain

$$\hat{H}_I(t) = -i\hbar g\left(\hat{\sigma}_+\hat{a}e^{-i\Delta t} - \hat{\sigma}_-\hat{a}^\dagger e^{i\Delta t}\right), \tag{121}$$

where $\Delta \equiv \omega - \omega_0$ is detuning.

Physically, RWA approach presumes that term $\hat{\sigma}_-\hat{a}$ corresponds to a downward transition in TLS accompanied by one-photon absorption. Term $\hat{\sigma}_+\hat{a}^\dagger$ describes

an elementary process of upward transition with the one-photon emission. These processes do not preserve the total number of photons, and, as a result, they are strongly suppressed.

Let us represent Hamiltonian $\hat{H}_{TLS}$ in (112) as

$$\begin{aligned} H_{TLS} = \frac{\hbar}{2}\begin{pmatrix} \omega_e + \omega_g & 0 \\ 0 & \omega_e + \omega_g \end{pmatrix} + \frac{\hbar}{2}\begin{pmatrix} \omega_e - \omega_g & 0 \\ 0 & \omega_g - \omega_e \end{pmatrix} = \\ = \frac{\hbar}{2}(\omega_e + \omega_g)\hat{\mathrm{I}} + \frac{\hbar}{2}(\omega_e - \omega_g)\hat{\sigma}_z, \end{aligned} \tag{122}$$

where $\hat{\mathrm{I}} = |e\rangle\langle e| + |g\rangle\langle g|$ is the unity operator. Again, we omit the first term in (122) relevant to constant energy. Summarizing and moving back into the Schrödinger picture we represent (112) as

$$\hat{H} = \frac{1}{2}\hbar\omega_0\hat{\sigma}_z + \hbar\omega\hat{a}^\dagger\hat{a} - i\hbar g\left(\hat{\sigma}_+\hat{a} - \hat{\sigma}_-\hat{a}^\dagger\right), \tag{123}$$

where $\omega_0 = \omega_e - \omega_g$. Eq. (123) establishes the JC model for TLS interaction with quantized cavity field. We represent (123) as

$$\hat{H} = \hat{H}_{ex} + \hat{H}_{eff}, \tag{124}$$

where

$$\hat{H}_{ex} = \hbar\omega\left(\hat{a}^\dagger\hat{a} + \frac{1}{2}\hat{\sigma}_z\right); \tag{125a}$$

$$\hat{H}_{eff} = -\frac{1}{2}\hbar\Delta\,\hat{\sigma}_z - i\hbar g\left(\hat{\sigma}_+\hat{a} - \hat{\sigma}_-\hat{a}^\dagger\right). \tag{125b}$$

From (124) with (125) it is easy to prove that excitation operator

$$\hat{N}_{ex} \equiv \hat{a}^\dagger\hat{a} + \frac{1}{2}\hat{\sigma}_z \tag{126}$$

commutes with $\hat{H}$, hence further we can work only with effective JC Hamiltonian (125b).

We consider the initial state of the total system as superposition

$$|\Psi(0)\rangle = \sum_{n=0}^{\infty} c_n|g\rangle|n\rangle, \tag{127}$$

where $|g\rangle|n\rangle$ establishes the tensor product (separable, non-entangled) state with the atom in ground state $|g\rangle$ and n photons in the quantum irradiation.

In (127), c_n is relevant to the initial photon probability distribution that we consider as Poissonian

$$|c_n|^2 = \frac{\bar{n}^n}{n!} e^{-\bar{n}}, \tag{128}$$

where $\bar{n}$ is a mean photon number. As shown in (57), probability $|c_n|^2$ corresponds to the initially coherent light field, $\bar{n} \equiv \langle \hat{n} \rangle$.

State (127) becomes entangled after temporal evolution:

$$|\Psi(t)\rangle = \sum_{n=0}^{\infty} [C_{g,n}(t)\, |g\rangle|n\rangle + C_{e,n}(t)\, |e\rangle|n\rangle], \tag{129}$$

where $C_{g,n} \equiv C_{g,n}(t)$ and $C_{e,n} \equiv C_{e,n}(t)$ are time-dependent probability amplitudes.

Before proceeding with state (129), it is instructive to examine its properties. For that we use interaction part $\hat{H}_I(t)$ of total Hamiltonian (123):

$$\hat{H}_I(t) = -i\hbar g \left(\hat{\sigma}_+ \hat{a} - \hat{\sigma}_- \hat{a}^\dagger \right). \tag{130}$$

The action of $\hat{H}_I$ on TLS ground state with n photons is

$$\begin{aligned} \hat{H}_I\, |g\rangle|n\rangle &= -i\hbar g \left(\hat{\sigma}_+ \hat{a}\, |g\rangle|n\rangle - \hat{\sigma}_- \hat{a}^\dagger \,\big|\, g\rangle|n\rangle \right) \\ &= -i\hbar g \sqrt{n}\, |e\rangle|n-1\rangle. \end{aligned} \tag{131}$$

In (131) we use Eqs. (10) and (118). Apparently, state $|g\rangle|0\rangle$ in (131) with no photons should be specified separately:

$$\hat{H}_I\, |g\rangle|0\rangle = 0, \tag{132}$$

where we explore definition (14) for vacuum state.

As it follows from Eqs. (131) and (132), the JC model provides coupling of state $|g\rangle|n\rangle$ with $|e\rangle|n-1\rangle$ leaving state $|g\rangle|0\rangle$ uncoupled. Thus, for the JC model we can recast (129) in a more suitable form:

$$|\Psi(t)\rangle = \sum_{n=1}^{\infty} [C_{g,n}\, |g\rangle|n\rangle + C_{e,n-1}\, |e\rangle|n-1\rangle] + C_{g,0}\, |g\rangle|0\rangle. \tag{133}$$

Since initial state (127) is a separable state of TLS ground state and cavity field,

$$C_{g,n}(0) = c_n, \quad C_{e,n-1}(0) = 0 \tag{134}$$

are the initial conditions for (133).

Inserting (129) into Schrödinger equation (91) with the Hamiltonian (125b), we obtain

$$\dot{C}_{g,n} = -i\frac{\Delta}{2}\, C_{g,n} + g\sqrt{n}\, C_{e,n-1}; \tag{135a}$$

$$\dot{C}_{e,n-1} = i\frac{\Delta}{2}\, C_{e,n-1} - g\sqrt{n}\, C_{g,n}. \tag{135b}$$

Thus, in Eqs. (135) we deal with a coupled pair of states, which effectively represent a simple two-state system.

The solution of (135) with (134) is the following:

$$C_{g,n}(t) = c_n \left(\cos[0.5\omega_{R,n}t] - i\frac{\Delta}{\omega_{R,n}} \sin[0.5\omega_{R,n}t] \right); \tag{136a}$$

$$C_{e,n-1}(t) = -c_n \frac{2g\sqrt{n}}{\omega_{R,n}} \sin[0.5\omega_{R,n}t], \tag{136b}$$

where $\omega_{R,n} = \sqrt{\Delta^2 + 4g^2 n}$ is the photon-number-dependent Rabi frequency, cf. (108).

To be more specific, let us examine (136) for atom-light resonance condition $\Delta = 0$. The probability to find the atom in ground state $|g\rangle$ is

$$P_g(t) = \sum_{n=0}^{\infty} |C_{g,n}(t)|^2 = \frac{1}{2} \sum_{n=0}^{\infty} |c_n|^2 \left(1 + \cos[2g\sqrt{n}t]\right), \tag{137}$$

where $|c_n|^2$ is defined in (128).

Eq. (137) establishes the quantum approach to Rabi oscillations when each photon number n contributes n quanta into Rabi oscillations with angular frequency $\Omega_{R,n} = 2g\sqrt{n}$. A semiclassical result may be obtained in the limit of large n when we suppose $n \approx \bar{n}$ and

$$\Omega_{R,n} \approx \Omega_{R,\bar{n}} \equiv 2g\sqrt{\bar{n}} \tag{138}$$

represents a mean Rabi frequency in the semiclassical limit. In this case, from (137) we immediately obtain

$$P_g(t) \approx \frac{1}{2} \left(1 + \cos[\Omega_{R,\bar{n}}t]\right). \tag{139}$$

Eqs. (139) and (138) lead to the relation obtained in (101) for population imbalance W that occurs for TLS in the presence of classical driving field.

In Fig. 8 we establish the behaviour of ground state probability $P_g(t)$ as a function of dimensionless time gt for a moderate average photon number. The envelope of $P_g(t)$ manifests atomic population periodical collapses and revivals, which represent an excellent example of a purely quantum phenomenon that occurs under the matter – light interaction. Collapses and revivals appear due to the interference between individual Rabi oscillators with their own Rabi frequencies $\Omega_{R,n}$, which depend on photon number n. The collapses result from the spread of the initial photon numbers.

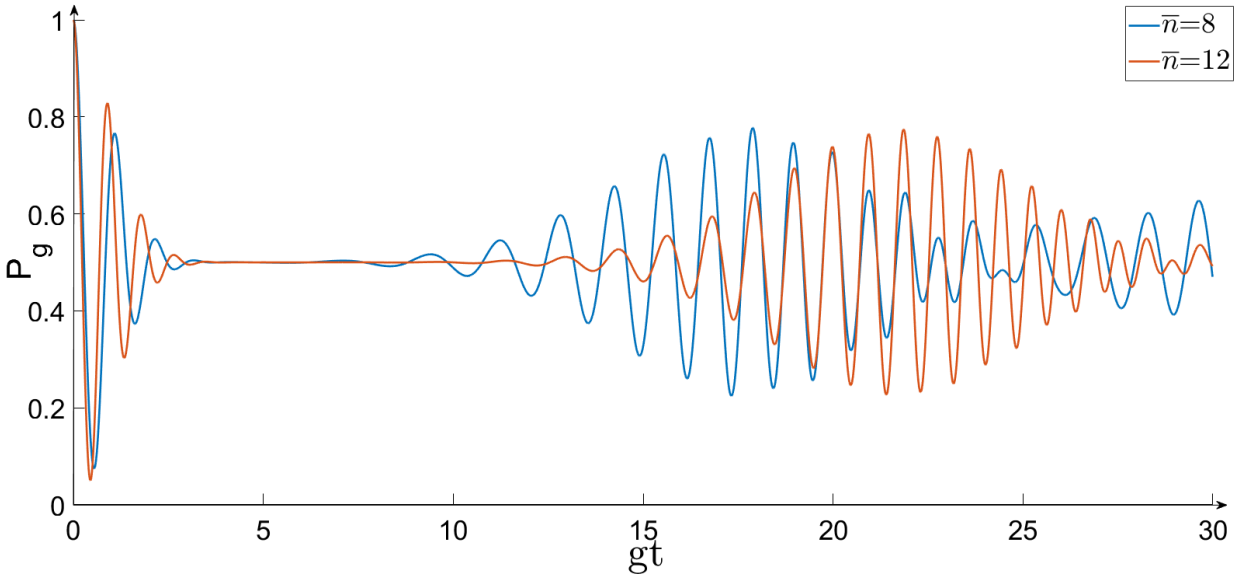

Fig. 8: Dependence of ground state probability P_g as a function of normalized time gt for the JC model with initially coherent light field

It is instructive to examine the limit of large mean photon number $\bar{n} \gg 1$ establishing $\sqrt{n}$ as

$$\sqrt{n} = \sqrt{\bar{n} + (n - \bar{n})} = \sqrt{\bar{n}} \sqrt{1 + \frac{n - \bar{n}}{\bar{n}}} \approx \sqrt{\bar{n}} \left(1 + \frac{n - \bar{n}}{2\bar{n}}\right). \qquad (140)$$

In (140) we expand $\sqrt{n}$ into a Taylor series, limiting ourselves by two terms. Then, we transfer to Gaussian probability distribution instead of the Poisson one:

$$\frac{\bar{n}^n}{n!} e^{-\bar{n}} \simeq \frac{1}{\sqrt{2\pi\bar{n}}} e^{-(n-\bar{n})^2/2\bar{n}} \qquad (141)$$

Combining (140), (141) with (137), we can find

$$P_g(t) = \frac{1}{2} + \frac{1}{2(2\pi\bar{n})^{1/2}} \int_{-\infty}^{+\infty} dn\, e^{-\frac{(n-\bar{n})^2}{2\bar{n}}} \cos\left[\Omega_{R,\bar{n}} t \left(1 + \frac{n-\bar{n}}{2\bar{n}}\right)\right], \quad (142)$$

where we extend the range of integration. Representing cosine in (142) as $\cos[...] = \frac{1}{2}(e^{i[...]} + e^{-i[...]})$, we can obtain the Fourier transform of a Gaussian function. After some straightforward calculations from (142) we arrive at

$$P_g(t) = \frac{1}{2}\left(1 + e^{-(t/\tau_{coll})^2} \cos[\Omega_{R,\bar{n}} t]\right), \quad (143)$$

where

$$\tau_{coll} = \frac{\sqrt{2}}{g} \quad (144)$$

determines the first collapse time.

Notably, τ_{coll} does not depend on average photon number $\bar{n}$ within the considered approach. From Fig. 8 it is clearly seen that envelopes of the blue and red curves vanish simultaneously.

The revivals occur when all the nearest-neighbor Rabi oscillators become in-phase again after initial dephasing. We can estimate the peak of the revival at time T_{rev}, at which the main number of Rabi oscillators described in (137) are in-phase. In other words, the revival occurs when the $\bar{n}$-th and the $(\bar{n}-1)$-th Rabi oscillators accumulate common phase

$$2g\sqrt{\bar{n}}\, T_{rev} - 2g\sqrt{\bar{n}-1}\, T_{rev} = 2\pi, \quad (145)$$

from which we obtain

$$T_{rev} = \frac{\pi}{g(\sqrt{\bar{n}} - \sqrt{\bar{n}-1})} \simeq \frac{2\pi\sqrt{\bar{n}}}{g}. \quad (146)$$

Eq. (146) completely agrees with the results shown in Fig. 8; in particular, T_{rev} grows with the average photon number increasing.

The practical importance of Eq. (146) may be elucidated if we use a semiclassical expression for Rabi splitting angular frequency $\Omega_{R,\bar{n}}$. Combining it with (138) we obtain

$$T_{rev} = \frac{4\pi\bar{n}}{\Omega_{R,\bar{n}}}. \quad (147)$$

From Eq. (147) it is clear that to experimentally observe the revivals we need a large mean Rabi frequency splitting obtained for moderate average photon number $\bar{n}$. Notice that the theory represented above does not take into account the effects of atomic decoherence and photon losses, which always appear in any scheme of quantum light – matter interaction. Thus, the observation of collapses and revivals in real world experiments is an important and non-trivial task; only a few experiments have been conducted.

4.2 Microcavity polaritons as coupled quantum matter-field states

The microcavity polaritons represent one more important exact solution of the matter – field interaction model. The model describes an ensemble of TLS placed in the cavity and interacting with quantized e.m. field. Practically, it may be obtained with semiconductor quantum wells (QWs) sandwiched by two distributed Bragg mirrors and placed in a Fabry-Perot microcavity, see Fig. 9. The exciton consisting of a bound electron-hole pair in a semiconductor quantum well represents an optically active dipole that occurs due to the Coulomb interaction between an electron in the conduction band and a hole in the valence band. Thus, for calculations we can recognize QW exciton as an effective TLS, which is strongly coupled with cavity field.

Microcavity photons have finite lifetime τ_{ph} due to the leakage of light through the Bragg mirrors. The strong coupling condition presumes that the inequalities

$$g \gg \frac{1}{\tau_{ph}},\ \gamma_0 \tag{148}$$

are fulfilled, where γ_0 is the TLS decoherence rate. In practice, we may consider that the system is in the strong-coupling regime if the excitation can coherently transfer between a photon and a TLS at least once.

In planar microcavity 2D excitons and 2D photonic modes can form new eigenmodes, which are called microcavity polaritons. We start with the Hamiltonian of the system in the RWA represented as (cf. [10])

$$\begin{gathered}\hat{H} = \hat{H}_F + \hat{H}_{ex} + \hat{H}_I \\ = \hbar \sum \Big(\omega(k)\, \hat{a}^\dagger_{\mathbf{k}} \hat{a}_{\mathbf{k}} + \omega_0(k)\, \hat{b}^\dagger_{\mathbf{k}} \hat{b}_{\mathbf{k}} + g\, (\hat{a}^\dagger_{\mathbf{k}} \hat{b}_{\mathbf{k}} + \hat{a}_{\mathbf{k}} \hat{b}^\dagger_{\mathbf{k}}) \Big),\end{gathered} \tag{149}$$

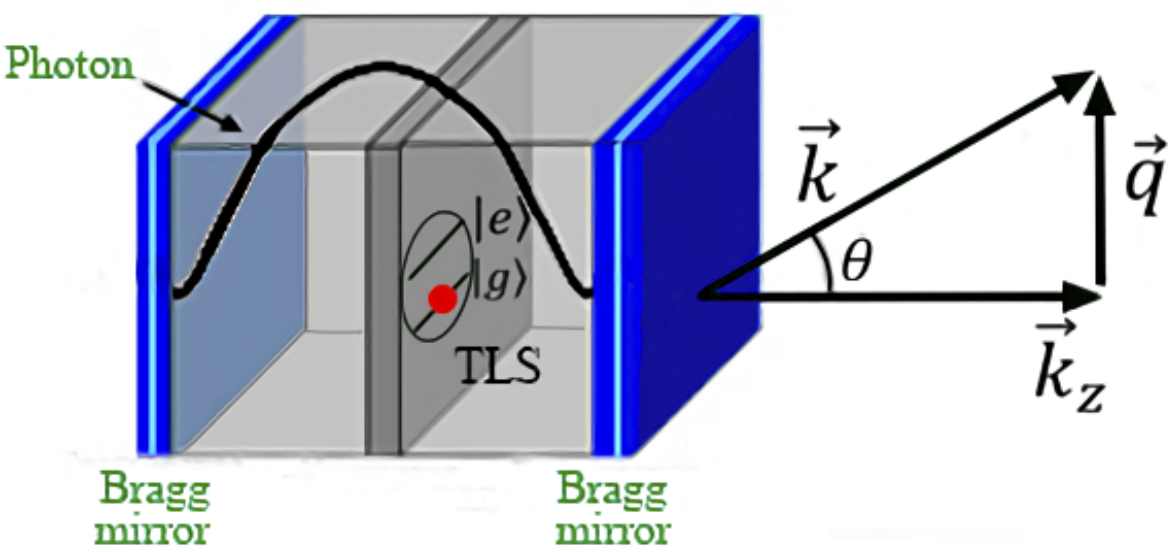

Fig. 9: Scheme of high quality planar microcavity containing quantum wells (QWs). QW exciton (TLS) in a planar microcavity couples with the photon mode possessing wave vector $\mathbf{k}$; k_z is a longitudinal component of field quantized in a microcavity. Photons are emitted at angle θ and correspond to polaritons possessing in-plane wave vector $\mathbf{q}$

where $\hat{a}^\dagger_{\mathbf{k}}$ ($\hat{b}^\dagger_{\mathbf{k}}$) is the photon (TLS excitation) creation operator with wavevector $\mathbf{k}$. Physically, we can understand TLS excitation, or simply exciton, as a TLS polarization. Thus, the sum in the brackets represents two linearly coupled oscillators.

Operators $\hat{a}_{\mathbf{k}}$, $\hat{a}^\dagger_{\mathbf{k}}$, $\hat{b}_{\mathbf{k}}$ and $\hat{b}^\dagger_{\mathbf{k}}$ satisfy the bosonic commutation relations

$$\left[\hat{a}_{\mathbf{k}},\, \hat{a}^\dagger_{\mathbf{k}'}\right] = \delta_{\mathbf{k}\mathbf{k}'}, \quad \left[\hat{b}_{\mathbf{k}},\, \hat{b}^\dagger_{\mathbf{k}'}\right] = \delta_{\mathbf{k}\mathbf{k}'}, \quad \left[\hat{a}_{\mathbf{k}},\, \hat{b}^\dagger_{\mathbf{k}'}\right] = 0. \tag{150}$$

In (149), $\omega(k)$ and $\omega_0(k)$ characterize the dispersion for optical field and TLS, respectively. For a planar microcavity they are

$$\omega(k) = c|\mathbf{k}| = c\sqrt{k_z^2 + q^2} \approx c\left(k_z + \frac{q^2}{2k_z}\right) = ck_z + \frac{\hbar q^2}{2m_{ph}}; \tag{151}$$

$$\omega_0(k) = \omega_0 + \frac{\hbar q^2}{2m_0}, \tag{152}$$

where q is a in-plane wave vector, k_z is a longitudinal wave number corresponding to the periodic boundary conditions upon the conventional field quantization.

In (151) we use a so-called ***paraxial approximation***, which is known from optics and relevant to the $|\mathbf{q}| \ll k_z$ condition. In this limit, it is possible to introduce effective photon mass in the cavity $m_{ph} = \hbar k_z/c$; m_0 is the TLS mass.

The Hamiltonian given by (149) can be diagonalized with the Bogoliubov transformation (which is unitary):

$$\hat{P}_{\mathbf{k}} = X_{\mathbf{k}}\hat{b}_{\mathbf{k}} + C_{\mathbf{k}}\hat{a}_{\mathbf{k}}; \tag{153a}$$

$$\hat{Q}_{\mathbf{k}} = -C_{\mathbf{k}}\hat{b}_{\mathbf{k}} + X_{\mathbf{k}}\hat{a}_{\mathbf{k}}, \tag{153b}$$

where $X_{\mathbf{k}}$ and $C_{\mathbf{k}}$ are Hopfield coefficients defined as

$$|X_{\mathbf{k}}|^2 = \frac{1}{2}\left(1 + \frac{\Delta_{\mathbf{k}}}{\sqrt{\Delta_{\mathbf{k}}^2 + 4g^2}}\right); \tag{154a}$$

$$|C_{\mathbf{k}}|^2 = \frac{1}{2}\left(1 - \frac{\Delta_{\mathbf{k}}}{\sqrt{\Delta_{\mathbf{k}}^2 + 4g^2}}\right). \tag{154b}$$

In (154) we define detuning $\Delta_{\mathbf{k}} = \omega_0(k) - \omega(k)$.

The operators in (153) obey commutation relations

$$\left[\hat{P}_{\mathbf{k}},\, \hat{P}^{\dagger}_{\mathbf{k}'}\right] = \delta_{\mathbf{k}\mathbf{k}'}, \quad \left[\hat{Q}_{\mathbf{k}},\, \hat{Q}^{\dagger}_{\mathbf{k}'}\right] = \delta_{\mathbf{k}\mathbf{k}'}, \quad \left[\hat{P}_{\mathbf{k}},\, \hat{Q}^{\dagger}_{\mathbf{k}'}\right] = 0, \tag{155}$$

where Hopfield coefficients $X_{\mathbf{k}}$ and $C_{\mathbf{k}}$ satisfy

$$|X_{\mathbf{k}}|^2 + |C_{\mathbf{k}}|^2 = 1. \tag{156}$$

The Hamiltonian diagonalization procedure presumes substitution of (153) with (154) into (149). Then, $\hat{H}$ becomes

$$\hat{H} = \hbar \sum_{\mathbf{k}} \Omega_{\mathrm{LP}}(k)\, \hat{P}^{\dagger}_{\mathbf{k}}\hat{P}_{\mathbf{k}} + \hbar \sum_{\mathbf{k}} \Omega_{\mathrm{UP}}(k)\, \hat{Q}^{\dagger}_{\mathbf{k}}\hat{Q}_{\mathbf{k}}. \tag{157}$$

Physically, operators ($\hat{P}_{\mathbf{k}}$,$\hat{P}^{\dagger}_{\mathbf{k}}$) and ($\hat{Q}_{\mathbf{k}}, \hat{Q}^{\dagger}_{\mathbf{k}}$) specified in (153) – (157) characterize new decoupled bosonic oscillators (eigenmodes), which are two types of quasiparticles resulting from the matter — field interaction; they are called upper (UP) and lower (LP) branch polaritons, respectively.

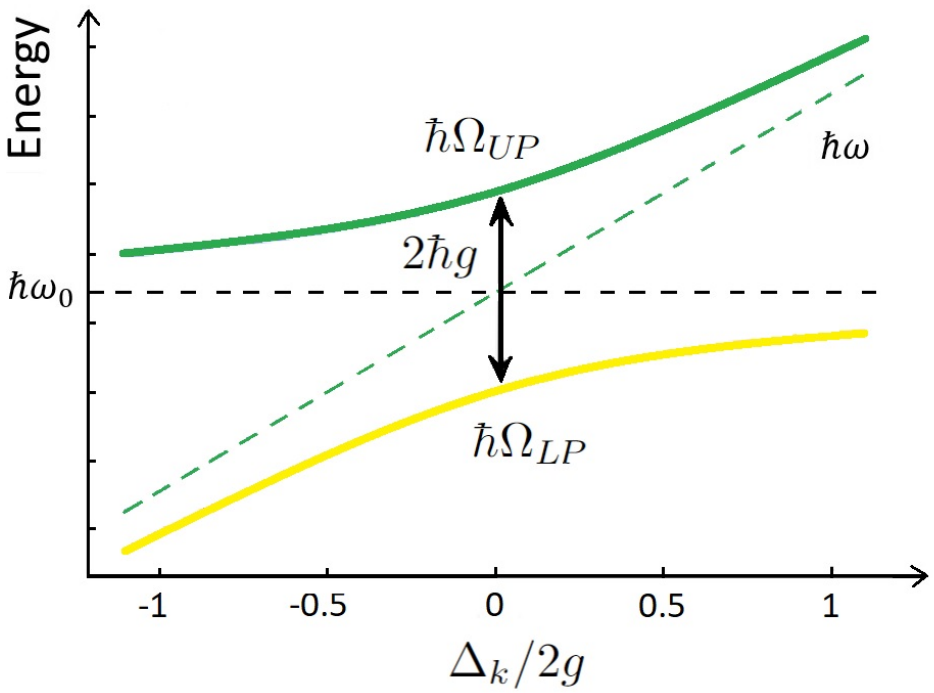

Fig. 10: Dependence of the upper and lower branch polariton energies (in arb. units) against normalized detunig $\Delta_{\mathbf{k}}/2g$ for in-plane momentum $q \simeq 0$. The dashed lines are relevant to photon and exciton (TLS) dispersions, separately

Characteristic angular frequencies $\Omega_{\rm UP}(k)$ and $\Omega_{\rm LP}(k)$ in (157) determine dispersion relation for upper and lower branch polaritons, respectively. They are derived within diagonalization procedure and may be represented as

$$\Omega_{\rm UP,\,LP}(k) = \frac{1}{2}\Big[\omega_0(k) + \omega(k) \pm \sqrt{4g^2 + \Delta_{\mathbf{k}}^2}\Big]. \qquad (158)$$

In Fig. 10 energies of upper and lower branch polaritons $\hbar\Omega_{\rm UP,LP}(k)$ (taken in arb. units) are shown as functions of detuning $\Delta_{\mathbf{k}}$. They demonstrate the anti-crossing effect, which is similar to the dependence for the dressed states in Fig. 6. The effect of anti-crossing for measured dispersions at different detunings represents important evidence of the strong coupling regime.

According to its definition (154), a polariton is a linear superposition of a TLS excitation and a photon. The fraction of photons and excitons adjusts by Hopfield coefficients $X_{\mathbf{k}}$, $C_{\mathbf{k}}$. From Eqs. (154) and Fig. 10 it is easy to see that in resonance, at $\Delta_{\mathbf{k}} = 0$, the coefficients are $|X_{\mathbf{k}}|^2 = |C_{\mathbf{k}}|^2 = \frac{1}{2}$, that implies LP and UP are exactly half-photon half-TLS excitation states. The gap between

upper and lower polariton branches is minimal and equal to $\Omega_{\rm UP}(k)-\Omega_{\rm LP}(k)=2g$, see Fig. 10.

On the contrary, in the limit of large detuning $|\Delta_{\mathbf{k}}|\gg g$, polaritons become photon-like or exciton-like, as follows from (153) and (154).

Now in (158), let us take into account cavity photon finite lifetime τ_{ph} and TLS excitation dephasing rate γ_0. In this limit characteristic angular frequencies $\Omega_{\rm UP}(k)$ and $\Omega_{\rm LP}(k)$ obtained in (158) should be modified. In the framework of the mean field theory, $\Omega_{\rm UP}(k)$ and $\Omega_{\rm LP}(k)$ are

$$\Omega_{\rm UP,\,LP}(k)=\frac{1}{2}\Big(\omega_0(k)+\omega(k)+i(\gamma_{ph}+\gamma_0) \pm\sqrt{4g^2+[\Delta_{\mathbf{k}}+i(\gamma_{ph}-\gamma_0)]^2}\Big), \tag{159}$$

where $\gamma_{ph}\simeq 1/\tau_{ph}$ is the cavity photon decay rate. From (159) it is evident that Rabi frequency may be suppressed in the presence of decoherence.

4.3 Features of in-plane polaritons

The polaritons with momentum $\mathbf{q}$, which appear parallel to cavity mirrors, are of special interest in quantum and condensed matter physics. Strong coupling between a microcavity photon and a TLS creates experimentally observable lower-polariton and upper-polariton dispersions, which possess minima at $\mathbf{q}=0$, see Fig. 11.

In this sense, in $\Delta_{\mathbf{k}}$ it is useful to separate the term independent on $\mathbf{q}$. In particular, with (151) and (152) we can represent it as

$$\Delta_{\mathbf{k}}=\Delta+\frac{\hbar q^2}{2m_0}-\frac{\hbar q^2}{2m_{ph}}, \tag{160}$$

where $q=|\mathbf{q}|$, $\Delta=\omega_0-ck_z$ is the detuning independent on the in-plane momentum, i.e. taken for $\Delta_{\mathbf{k}}$ at $\mathbf{q}=0$.

For a given Δ, Eq. (158) establishes the dispersion of in-plane polaritons. In the paraxial approximation, for $\hbar q^2/2m_{ph}\ll g$, the dispersion relation reads as

$$\Omega_{\rm LP,\,UP}(q)=\Omega_{\rm LP,\,UP}(q=0)+\frac{\hbar q^2}{2m_{\rm LP,\,UP}}, \tag{161}$$

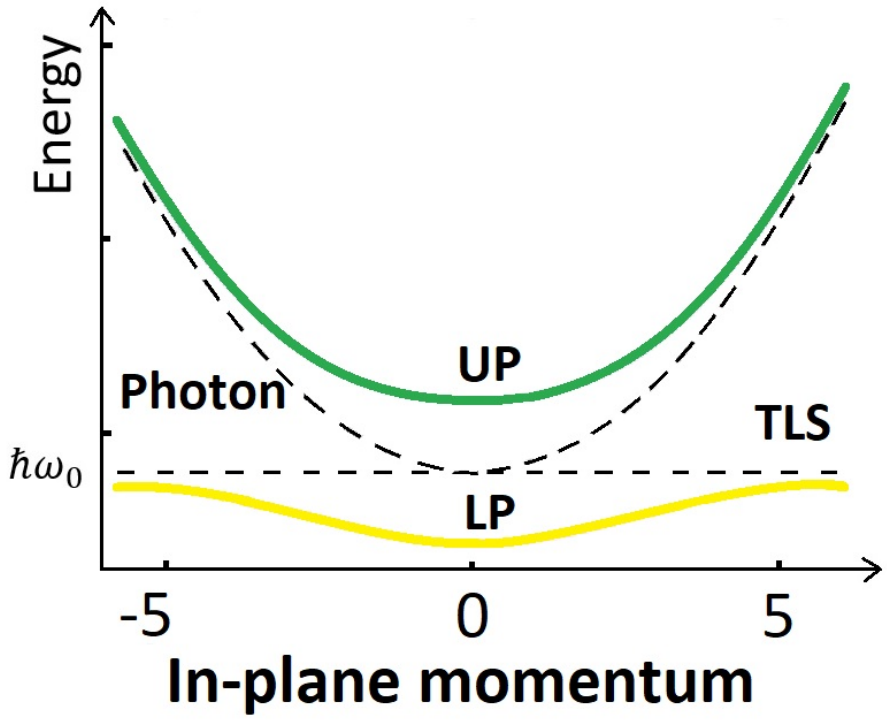

Fig. 11: Dependence of in-plane polariton energy against momentum $\hbar q$ for $\Delta = 0$. The strong coupling between the cavity photon and QW excitons splits the dispersions near $q = 0$ and creates the lower polariton (LP) and upper (UP) polariton branches. The cavity photon and exciton dispersions are given in (151) and (152), respectively

where m_{LP} and m_{UP} are effective masses of lower and upper branch polaritons, respectively. They may be found as

$$m_{\mathrm{LP,\,UP}} = \frac{2m_0 m_{ph}\sqrt{\Delta^2 + 4g^2}}{(m_0 + m_{ph})\sqrt{\Delta^2 + 4g^2} \pm (m_0 - m_{ph})\Delta}. \tag{162}$$

It is worth noting that the uncoupled cavity photon dispersion is parabolic, see (151) and Fig. 11. The dispersion of QW excitons is also parabolic and characterized by (152). However, m_0 is $4 - 5$ orders larger than the effective photon mass, and condition

$$m_{ph} \ll m_0 \tag{163}$$

is satisfied within real-world experiments with exciton-polaritons for the modest values of detuning Δ. Thus, in Fig. 11 we can assume that $\omega_0(k) \approx \omega_0 = const$.

However, at large enough detuning $|\Delta|$, where $|\Delta| \gg g$, the dispersions of the lower and upper branch polaritons match to the exciton and photon dispersions (161), respectively.

It is important that for resonant matter – field interaction we can put $\Delta = 0$ in (162) and obtain

$$m_{\mathrm{LP,\,UP}} = \frac{2m_0\, m_{ph}}{m_0 + m_{ph}}. \tag{164}$$

In the limit of (163) from (164) we obtain

$$m_{\mathrm{LP,\,UP}} \approx 2m_{ph}. \tag{165}$$

Eq. (165) establishes effective polariton mass close to the resonance condition. One can see that in this useful limit polaritons represent small-mass quasiparticles. The small effective mass of lower-branch polaritons makes them promising for observation phase transitions and Bose-Einstein condensation at high (room) temperatures.

Today, typical high-quality semiconductor microcavities possess $\gamma_{ph}^{-1} = 1-10$ ps and more, $\gamma_0^{-1} \simeq 0.1-1$ ns. Thus, the polariton lifetime is mainly determined by the cavity photon lifetime. Loosely speaking, condition

$$\gamma_0 \ll \gamma_{ph} \ll g \tag{166}$$

is satisfied in current experiments with exciton-polariton BEC observation. Since polaritons appear in 2D system, they require a special trapping potential. Such a potential can be created by either semiconductor sample modification or choice of the pump beam special profile, for more detail see [10].

4.4 Problems

1. Prove commutation relations (119).

2. Consider cesium two-level atom placed in Fabry-Perot cavity of length $60\,\mu m$ and modal volume $5 \times 10^{14}\, m^3$. The cavity mode is tuned to resonance with atomic transition at $852\, nm$ which has $\wp_{ge} = 3 \times 10^{29}\, C \cdot m$. Estimate numerically atom-field coupling constant g, cf. [2].

Answer: $g = 1.5 \times 10^8\, rad/s$.

3. Consider the Hermitian spin operators as follows

$$\hat{\sigma}_x = \hat{\sigma}_+ + \hat{\sigma}_-; \tag{167a}$$

$$\hat{\sigma}_y = i(\hat{\sigma}_- - \hat{\sigma}_+). \tag{167b}$$

Find the matrix representation for $\hat{\sigma}_{x,y,z}$ operators.

4. Prove SU(2) algebra commutation relations

$$[\hat{\sigma}_x,\, \hat{\sigma}_y] = 2i\hat{\sigma}_z, \quad [\hat{\sigma}_z,\, \hat{\sigma}_x] = 2i\hat{\sigma}_y, \quad [\hat{\sigma}_y,\, \hat{\sigma}_z] = 2i\hat{\sigma}_x. \tag{168}$$

5. Prove that the operator representing the total number of quanta,

$$\hat{N} = \hat{a}^\dagger \hat{a} + \hat{\sigma}_+ \hat{\sigma}_-, \tag{169}$$

commutes with the Hamiltonian (125b).

6. Derive the right part of (146).

7. Derive Eqs. (136), (137) for nonzero detuning Δ. Analyze separatly the limit of $|\Delta| \gg g$. Analize the effect of $\Delta \neq 0$ on the times of collapses and revivals. Plot them.

8. Examine the mean values of spin operators $\langle \Psi(t)|\hat{\sigma}_{x,y,z}|\Psi(t)\rangle$ using (133), (168).

9. Derive uncertainty relations from (168). Examine variances of spin operators $\left\langle (\Delta\hat{\sigma}_{x,y,z})^2 \right\rangle$ for JC state (133).

10. In experiments with atoms placed in the cavity at low atomic-beam flux, the cavity contains essentially-thermal photons. They obey Bose-Einstein statistics possessing probability distribution

$$|c_n|^2 = \frac{\bar{n}^n}{(1+\bar{n})^{n+1}}, \tag{170}$$

where $\bar{n} = \left(e^{\hbar\omega/k_B T} - 1\right)^{-1}$ is a mean thermal photon number.

Examine ground state population Eq. (137) with the probability determined by (170) and plot the depences obtainde. Compare the collapses and revivals

quantum phenomenon for thermal and coherent fields.

11. Prove that Bogoliubov transformation (154a), (154b) is a unitary transformation without losses in a general case.

12. Estimate numerically effective photon mass m_{ph} in the cavity, which corresponds to cavity field frequency $\omega/2\pi = 353\text{THz}$. How many times is it smaller than the free electron mass?

13. Derive (157) performing the Hamiltonian (149) diagonalization procedure.

14. Prove that Eq. (162) may be obtained from quasiparticle effective mass definition

$$m_{\text{UP, LP}} = \hbar \left(\frac{\partial^2 \Omega_{\text{UP, LP}}(k)}{\partial q^2}\bigg|_{q=0} \right)^{-1}. \tag{171}$$

15. Consider (162) in large detuning limit $|\Delta| \gg g$. Find approximate expressions for polariton masses $m_{\text{UP, LP}}$. Examine positive and negative detuning Δ limits.

16. Consider group velocity of polaritons

$$\text{V}_{\text{UP, LP}} = \frac{\partial \Omega_{\text{UP,LP}}(k)}{\partial q}. \tag{172}$$

Examine (172) in the limits of $\Delta = 0$ and $|\Delta| \gg g$. Consider positive and negative detuning Δ limits.

17. Prove that the lifetime of polaritons may be obtained in the form

$$\gamma_{\text{LP}} = |X_{\mathbf{k}}|^2 \gamma_0 + |C_{\mathbf{k}}|^2 \gamma_{ph}; \tag{173a}$$

$$\gamma_{\text{UP}} = |C_{\mathbf{k}}|^2 \gamma_0 + |X_{\mathbf{k}}|^2 \gamma_{ph}. \tag{173b}$$

Examine (173a), (173b) in two limiting cases, which are $\Delta = 0$ and $|\Delta| \gg g$, respectively. Consider positive and negative detuning Δ limits.

18. The Hamiltonian of matter-field interaction beyond RWA may be described as (cf. (149))

$$\hat{H} = \hbar \sum \Big(\omega(k)\, \hat{a}^\dagger_{\mathbf{k}} \hat{a}_{\mathbf{k}} + \omega_0(k)\, \hat{b}^\dagger_{\mathbf{k}} \hat{b}_{\mathbf{k}} + g\, (\hat{a}^\dagger_{\mathbf{k}} + \hat{a}_{\mathbf{k}})(\hat{b}_{\mathbf{k}} + \hat{b}^\dagger_{\mathbf{k}}) \Big), \tag{174}$$

Diagonalize (174) finding eigenfrequencies and eigenmodes (polaritons).

5 Guidelines for Practical Work

5.1 Practice work report template

PRACTICAL WORK REPORT `No`
`"Title of the Practical Work"`

Student's Name and Surname, Group No.

1. The aim of the work;
2. Objectives of the work;
3. The course of work;
4. Input Data/Analysis/Results/Discussion;
5. Conclusion;
6. References.

5.2 Requirements

– correct processing of measurement results;

– the report is comprehensive and presents the material in a logical and coherent way;

– all the necessary sections are included;

– all the necessary plots are presented;

– all the control questions are answered correctly.

5.3 Grading scale and evaluation criteria

Each practical work is evaluated based on a scale from 4 to 8 points, which gives a total maximum of 40 points for five practical works.

8 points: all tasks are completed, all control questions are answered clearly and correctly.

6-7 points: all tasks are completed with minor errors that do not affect the resultant correct answer; all control questions are answered with the teacher's comments.

3-5 points: not all tasks are completed correctly; all control questions are answered with the teacher's comments.

1-3 points: all taskes are failed; the student answers the control questions with errors or does not answer the control questions at all.

If the student fails to report on a practical work, they receive 0 points.

6 Bibliography

[1] V.B. Berestetskii, E.M. Lifshitz, and L.P. Pitaevskii. *Quantum Electrodynamics: Course of Theoretical Physics*, volume 4. Butterworth-Heinemann; 2nd edition, 1982.

[2] Mark Fox. *Quantum Optics*. Oxford University Press, 2006.

[3] Rodney Loudon. *The Quantum Theory of Light*. Oxford University Press, 2000.

[4] S.M. Barnett and P.M. Radmore. *Methods in Theoretical Quantum Optics*. Clarendon Press, Oxford, 1997.

[5] C. Gerry and P. Knight. *Introductory Quantum Optics*. Cambridge University Press, 2005.

[6] S.A. Akhmanov and S.Yu. Nikitin. *Fizichyeskaya optika: Uchyebnik*. Izd-vo Mosk.Univ.: Nauka; 2nd edition, 2004.

[7] B. Yurke, S.L. McCall, and J.R. Klauder. Su(2) and su(1,1) interferometers. *Physical Review A*, 33:4033, 1986.

[8] M. Scully and S. Zubairy. *Quantum Optics*. Cambridge University Press, 1997.

[9] C. Cohen-Tannoudji, J. Dupont-Roc, and G. Grynberg. *Atom-Photon Interactions. Basic Processes and Applications*. WILEY-VCH Verlag GmbH Co. KGaA, Weinheim, 2004.

[10] H. Deng, H. Haug, and Y. Yamamoto. Exciton-polariton bose-einstein condensation. *Rev. Mod. Phys.*, 82:1489, 2010.

Алоджанц Александр Павлович
Баженов Андрей Юрьевич
Никитина Мария Михайловна
Осипов Степан Валерьевич
Царёв Дмитрий Владимирович

INTERACTION OF RADIATION WITH MATTER: GUIDELINES FOR PRACTICAL WORK

Учебное пособие

В авторской редакции
Редакционно-издательский отдел Университета ИТМО
Зав. РИО Н.Ф. Гусарова
Подписано к печати
Заказ №
Тираж
Отпечатано на ризографе

Редакционно-издательский отдел
Университета ИТМО
197101, Санкт-Петербург, Кронверкский пр., 49, литер А